Available online at www.sciencedirect.com
ScienceDirect
ELSEVIER
Quaternary International ▮ (▮▮▮▮) ▮▮▮–▮▮▮
INQUA 1928

Mid-distal occurrences of the Albano Maar pyroclastic deposits and their relevance for reassessing the eruptive scenarios of the most recent activity at the Colli Albani Volcanic District, Central Italy

Biagio Giaccio[a,*], Andrea Sposato[a], Mario Gaeta[b], Fabrizio Marra[c], Danilo M. Palladino[b], Jacopo Taddeucci[c], Mario Barbieri[b], Paolo Messina[a], Mario F. Rolfo[d]

[a]*Istituto di Geologia Ambientale e Geoingegneria, CNR, Via Bolognola 7, 00138 Rome, Italy*
[b]*Dipartimento di Scienze della Terra, Università di Roma "La Sapienza", Rome, Italy*
[c]*Istituto Nazionale di Geofisica e Vulcanologia, Rome, Italy*
[d]*Dipartimento di Storia, Università di Roma "Tor Vergata", Rome, Italy*

Abstract

The Late Pleistocene Albano Maar hosted the most recent volcanic activity of the Colli Albani Volcanic District, represented at near-vent sections by a thick pyroclastic succession of seven units clustered in two main eruptive cycles dated at around 70–68 and 41–36 ka B.P., respectively. Recent stratigraphic investigations allowed us to recognise a pyroclastic succession comprising four eruptive units widely spread in the northeastern sectors of the Colli Albani volcano, up to 15 km eastward from the Albano Maar. Integrated tephrostratigraphic, morpho-pedostratigraphic, archaeological, petrological and geochemical analyses enable us to recognise them as distal deposits of the first, third, fifth and seventh Albano Maar eruptions, enlarging significantly their previously supposed dispersion area. Further tephrostratigraphic studies in central Apennine area, allowed us to identify the Albano Maar products in Late Pleistocene deposits of several intermountain basins, extending still further the dispersion area of distal ash fallout as far as 100–120 km from the vent. On the basis of the identification and the study of these previously unrecognised mid-distal Albano Maar deposits, a reappraisal of the eruptive scenarios and related energetic parameters is proposed.

1. Introduction

A growing body of geo-volcanological and geochronological evidence points out that the Albano multiple maar (Fig. 1) hosted the most recent eruptive activity in the Colli Albani Volcanic District documented up to now (De Rita et al., 1995a; Villa et al., 1999; Karner et al., 2001; Funiciello et al., 2002, 2003; Marra et al., 2003; Soligo et al., 2003; Giordano et al., 2006; Freda et al., 2006a, b). Although strong disagreement still subsists on its eruptive history and in particular about the age of the last eruptive episode, the dating of which flouts between c. 5 ^{14}C ka B.P. (Funiciello et al., 2002, 2003) and c. 36 ka B.P. (Freda et al., 2006a, b), according to these recent studies the Colli Albani volcanic area should be now reclassified as an active, or at least quiescent, volcano.

Crucial as it is in a hazard evaluation prospective, here we do not report new relevant, required data to address the problem of the time recurrence of the Albano Maar explosive eruptions. For the purpose of the present study, we refer to the most complete available chronological framework recently acquired through ^{40}Ar/^{39}Ar measurements (Freda et al., 2006a; Table 1). Indeed, our study principally deals with the identification of the largest eruptive episodes and the reconstruction of related eruptive/post-eruptive scenarios, intensities and magnitudes, which are as much relevant for the hazard assessment from possible eruptive unrest in the future.

Since relatively distal settings are more suitable than proximal ones in order to recognise higher-intensity explosive events, one of the main aim of this study is the improving of the knowledge on the distal occurrences of

*Corresponding author. Tel.: +39 06 8807 0063; fax: +39 06 880 4463.
E-mail address: biagio.giaccio@igag.cnr.it (B. Giaccio).

1040-6182/$ - see front matter © 2006 Published by Elsevier Ltd.
doi:10.1016/j.quaint.2006.10.013

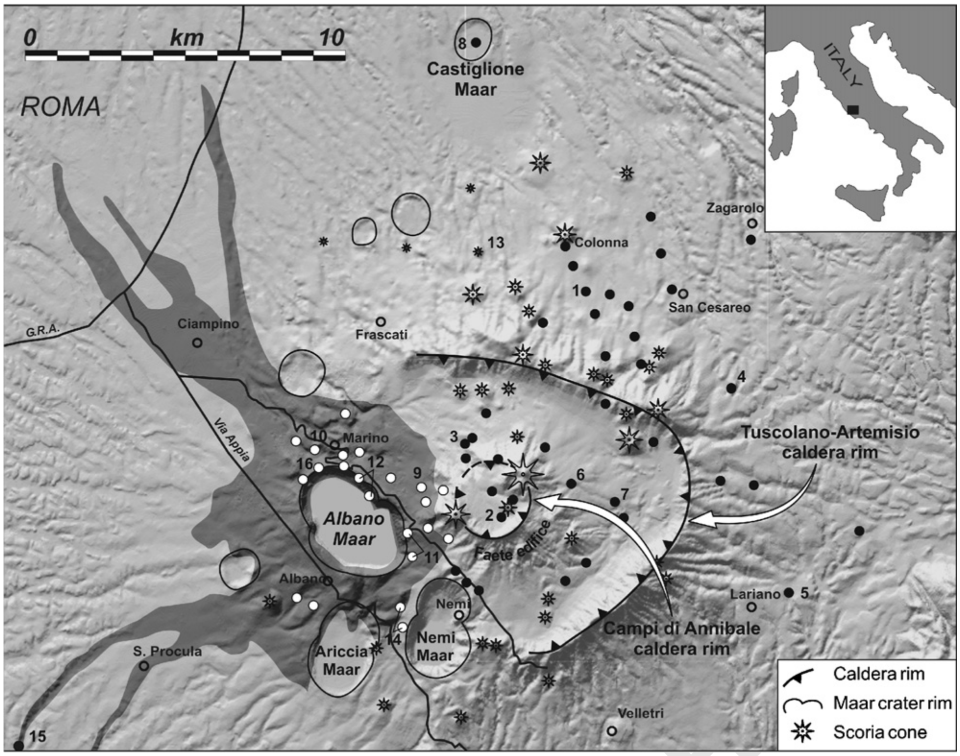

Fig. 1. The Albano multiple Maar and its products within the context of the Colli Albani Volcanic District. Shaded area: map of the dispersion area of the Albano pyroclastic deposits, including possibly reworked products, as reported in previous studies (data from De Rita et al., 1988, 1995a, b; Funiciello et al., 2002; Giordano et al., 2002a; Freda et al., 2006a). White dots: investigated sections within the proximal area; black dots: occurrences of mid-distal pyroclastic deposits correlated to the Albano Maar units. Numbers refer to sections mentioned in the text.

Table 1
Schematic stratigraphic succession and age of the proximal pyroclastic products of the Albano Maar correlated with their distal equivalent units (DUs)

Proximal area				Distal area (NE)
De Rita et al. (1995a)	Freda et al. (2006a, b) (with updating)			This study
Stratigraphy	$^{40}Ar/^{39}Ar$ age (ka B.P.)	Eruptive cycles	Stratigraphy	Stratigraphy
V Unit *Peperino Albano*			Present, deep soil	Present, deep soil
	35.9±0.6		Unit ***f***	Albano DU4
			Incipient paleosol	Shallow paleosol
	36.1±0.3		Unit ***e***	
	40.9±0.8	Late	Lapis Albanus	
			Incipient paleosol	
			Unit ***d***	Albano DU3
Paleosol			Moderately deep paleosol	Deep paleosol
IV Unit	41.2±1.1		Unit ***c***	
Paleosol			Deep paleosol	
III Unit	68.6±1.1		Unit ***b***	Albano DU2
Paleosol			Shallow paleosol	Shallow paleosol
II Unit		Early	Unit $\boldsymbol{b}_\alpha$	
Paleosol			Shallow paleosol	
I Unit	69.4±0.6		Unit ***a***	Albano DU1
			Very deep paleosol on Faete Phase or Ariccia Maar products	Very deep paleosol on Faete Phase products

A comparison with previous stratigraphic subdivision of De Rita et al. (1995a) is also shown.

the Albano eruptive products. The recognition and correlation of the Albano eruptive products, from near vent sections to mid-distal area, is in fact a crucial point for the reconstruction of the areal dispersal and determination of relevant eruptive parameters (i.e. erupted volumes, eruption column heights, mass discharge rates) for major explosive events.

In this regard, previous studies focused on the reconstruction of the Albano Maar stratigraphy mostly in very proximal (near-vent) locations and revealed a complex activity history related to multiple eruptive centres clustered in the present lake area (e.g. De Rita et al., 1995a; Freda et al., 2006a). Until now, more distal Albano deposits have been recognised only in limited areas north and south-west of the crater (Fig. 1) (Funiciello et al., 2002, 2003; Giordano et al., 2002b; Freda et al., 2006a). Moreover, in this area the Albano deposits are predominantly represented by channelled lithofacies, from primary and secondary volcaniclastic currents, of volcanological, tephrostratigraphic and tephrochronological controversial interpretation (e.g. see Funiciello et al., 2003; Marra and Karner, 2005 for two different accounts). Therefore, despite the advances in the reconstruction of its recent hydromagmatic activity, the present knowledge on the mid-distal products of the Albano Maar is still unsatisfactory for an adequate assessment of the related eruptive parameters and scenarios.

Here, we present new and re-interpreted data on previously unrecognised mid-distal occurrence of the Albano pyroclastic products, which can be now traced over a much wider area than previously mapped. These data provide the stratigraphic basis, which enables us to assess or reappraise the eruptive dynamics related to the most recent explosive volcanic activity of the Colli Albani Volcanic District, with obvious significant implications in terms of expectable future events and hence of assessment of the related hazard.

2. The Albano Maar

2.1. Geo-volcanological setting

The Albano Maar (Fig. 1) belongs to the Colli Albani Volcanic District of the ultrapotassic Roman Province, developed along the Tyrrhenian margin during the Middle/Upper Pleistocene (e.g. Peccerillo, 2001; Marra et al., 2004 and reference therein).

The Colli Albani volcanic history may be roughly subdivided in three main phases characterised by volumetrically and dynamically different eruptive events (e.g. De Rita et al., 1988, 1995a; Giordano et al., 2006). The early Tuscolano-Artemisio Phase (c. 561–351 ka B.P.; Karner et al., 2001) was, to a great extent, the most explosive and voluminous one, as testified by at least five large pyroclastic flow-forming eruptions and minor effusive activity. This phase ended with a caldera collapse followed by intra- and peri-caldera effusive and strombolian activity of numerous scoria cones, mostly aligned along the Tuscolano-Artemisio caldera rim. The second phase of activity (Faete Phase, c. 308–250 ka B.P; Marra et al., 2003), started with peripheral effusive eruptions coupled with the hydromagmatic activity of several tuff rings localised on the northern slope of the Tuscolano-Artemisio, and ultimately led to the formation of the Faete central edifice and of several minor scoria cones within the intra-caldera area. The third Late Hydromagmatic Phase (c. 200–36 ka; Marra et al., 2003) was dominated by pyroclastic surge eruptions, with formation of several monogenetic or multiple maars and/or tuff rings clustered southwest of the Mt. Faete edifice (Fig. 1).

2.2. Stratigraphy and chronology

The Albano Maar documented the most voluminous and recent activity (70–36 ka; Freda et al., 2006a) of Late Hydromagmatic Phase. It was previously described as a multiple tuff ring (De Rita et al., 1995a, b), the activity of which consisted of five main explosive cycles. The fifth eruption cycle of Albano emplaced a pyroclastic-flow deposit, interpreted as a phreatomagmatic basic ignimbrite (Giordano et al., 2002a), which is the most famous deposit of Albano, as it was quarried since the IV Century B.C. by the ancient Roman builders and extensively used under the name of Lapis Albanus; it is known in literature also as "Peperino di Marino" or "Peperino Albano".

More recently, Freda et al. (2006a, b) and Giordano et al. (2006) recognised seven eruptive units separated by six, more or less developed paleosols (PSs). In particular, Freda et al. (2006a) provided a detailed description of the stratigraphy of the proximal sections, a tentative correlation with mid-distal deposits, and a geochronologic framework, acquired through 13 40Ar/39Ar datings of as many volcanic layers. According to this study the eruptive history of the Albano Maar can be dividend into two main, geochronologically distinct eruptive cycles, at 69 ± 1 ka and at 39 ± 1 through 36 ± 1 ka, respectively (Table 1).

The first, Early cycle produced the lower, more than 60 m thick, suite of deposits at the Albano Lake proximal section. Two incipiently pedogenized ash layers divide this portion of the succession, indicating the presence of three separate eruptions (i.e. units ***a***, $\boldsymbol{b}_\alpha$ and ***b***; Fig. 2) that occurred in a relatively short time interval, as inferred from 40Ar/39Ar dating of the lowest and of the uppermost units, which yielded statistically indistinguishable ages of 69.4 ± 0.6 and 68.6 ± 1.1 ka, respectively (Freda et al., 2006a, Table 1). A thick horizon of altered ash capped by a pedogenized layer occurs at the top of unit ***b***, according to the ~30 kyr-long dormancy that separated the first and the second eruptive cycles (Table 1).

At Albano Lake and other near vent sections, three shallow, incipient PSs divide the products of the second, Late cycle into four different eruptions (units ***c***, ***d***, ***e*** and ***f***; Fig. 2), spanning a slightly larger temporal interval between c. 41 ka, age of the oldest unit ***c***, and c. 36 ka of the uppermost and last recognised unit ***f*** (see Table 1 for details). Previous ^{14}C determinations on unburnt wood fragments embedded in the "Peperino Albano" deposits yielded an age of c. 29–30 ^{14}C ka B.P. (Fornaseri and Cortesi, 1989), roughly equivalent at 34–35 cal ka B.P. (e.g. Fairbanks et al., 2005).

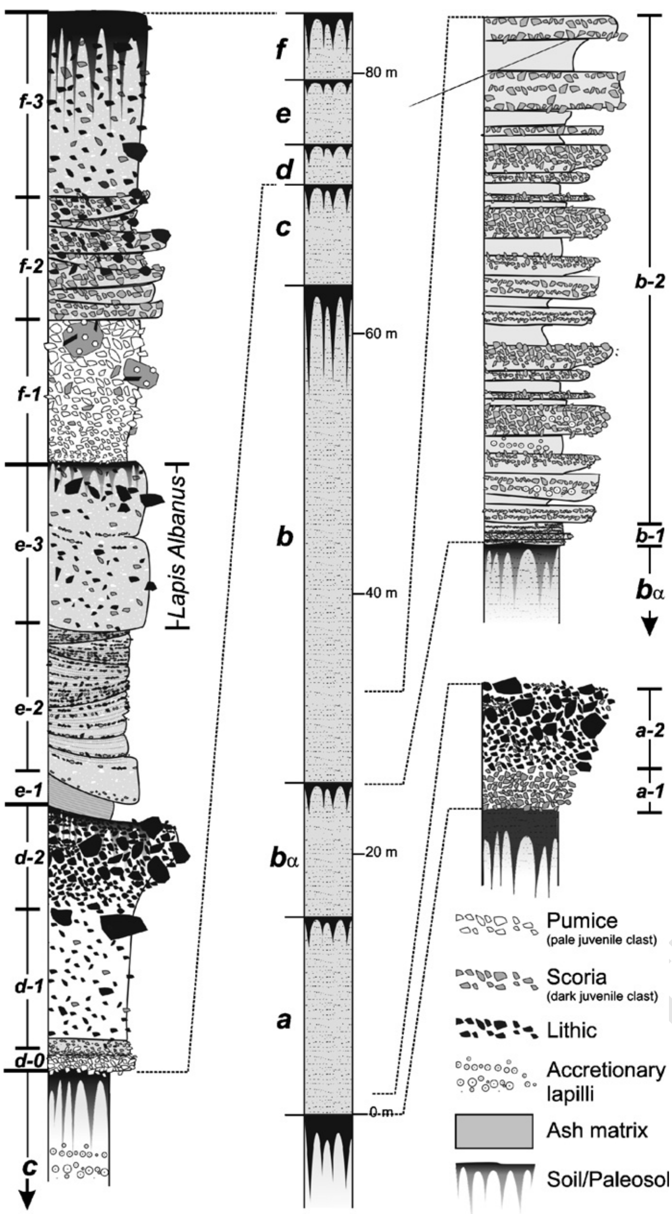

Fig. 2. Schematic, comprehensive stratigraphic succession of the seven Albano Maar proximal units with some more detailed logs related to the most distinctive units and/or subunits.

2.3. *Main stratigraphic, petrological and geochemical markers*

To establish reliable tephrostratigraphic correlation is a crucial task for the purpose of present study. This in turn is depending on the recognition of distinctive stratigraphic, textural, petrological and geochemical characters that allow to trace the pyroclastic deposits from the near vent sections to the distal ones. In the light of the available data from literature, mostly provided by the recent study of Freda et al. (2006a, b), and on the basis of new field, petrological and geochemical investigations carried out on several proximal sections (Fig. 1), we recognised within the Albano succession some useful markers for reliable tephrostratigraphic correlations.

The most distinctive layers occur within the suite of the Late eruptive cycle, more precisely within unit ***d*** and ***f*** (Fig. 2). Unit ***d*** shows at its base a thin layer of well vesicular and aphiric white pumice lapilli (layer ***d*–0**), a type of juvenile clasts virtually unique within the whole geological record of the Alban Hills volcano. Quite distinctive is also the well-sorted, clast-supported, lithic- and crystal-rich layer which occurs at top of this unit (layer ***d*–2**). The concurrence of both the layers, indeed makes the unit ***d*** one of the most distinctive pyroclastic deposits among the seven units of the Albano Maar suite.

As much idiosyncratic are the internal texture and the characters as a whole of the juvenile components characterising the two lowermost layers of the uppermost unit ***f***. The basal layer ***f*–1** is a dm- to m-thick fall deposit of cm-sized yellowish pumiceous clasts including, out-sized, porphiritic, green-black scoria blocks, characterised by cm-large crystals of leucite and dark mica and by sub-mm-sized crystals of hauyna. At most proximal sections (e.g. Palazzolo; site 11 in Fig. 1), the largest scoria clasts reach the diameter of a metre or more, and the same, peculiar juvenile clasts occur in the overlaying layer (***f*–2**) showing low-angle cross stratification (Fig. 2).

Among the three units of the Early eruptive cycle, the most distinctive lithostratigraphic and textural characters occur at the base of unit ***b*** (Fig. 2). At very proximal outcrops, the basal subunit ***b*–1** includes a cm-thick, well sorted, clast-supported level enclosed between two, cm-thick fine ash layers. At short distance from the vent the same unit is a dm-thick clast-supported fallout deposits of cm-sized orange scoria with a symmetric grading, reverse to normal upward. Ubiquitously, subunit ***b*–1** is overlaid by a well lithified, dark grey deposit of repeated cm- to dm-thick, plane-parallel beds of cemented ash matrix enclosing poorly vesiculated, rounded, both dark and orange scoria clasts, lava fragments, and sparse accretionary lapilli (layer ***b*–2**; Fig. 2) mostly reversely graded. The black scoria clasts include abundant sub-mm-sized leucite crystals imparting them a peculiar textural character. Intercalated at different heights in unit ***b***, a number of scoria fallout levels also appear (subunits ***b*–3**, **4**, **11**, **12**, and **13**).

We also take into account as useful marker layers the fallout deposit at the base of unit ***a*** (***a*–1**), made up of cm-sized, poorly visiculated black-brown scoria, and the overlying breccia level (***a*–2**) mostly containing dm-sized lithic clasts of volcanic (lava) and sedimentary (clay) origin (Fig. 2). Noteworthy, among the juvenile scoria clasts of the whole Albano series, only those occurring in the unit ***a***, in addition to the ubiquitous crystals of clinopiroxene, leucite and mica, contain a significant amount of olivine, making quite straightforward the recognition of this unit.

From the chemical composition point of view, by using the most common classification grid of the Total Alkali Silica diagram, the Albano Maar pyroclastics plot mostly within the foidite/phono-tephrite field (Freda et al., 2006a).

This is the most common composition of the Colli Albani volcanic rocks (e.g. Trigila et al., 1995), and hence the former would seem chemically hardly distinguishable. However, recent studies (Freda et al., 2006a) indicate that the glasses of juvenile scoria of uppermost unit ***f*** have a relative high content in Na_2O ($>5\%$) and a K_2O/Na_2O ratio barely greater than 1. This is a singular, very peculiar chemical character for the Colli Albani rocks, which commonly show a low Na_2O concentration and a very high alkali ratio (e.g. Trigila et al., 1995). Our additional chemical analyses of the glass of juvenile clasts from subunit ***f*–1** confirm this singular composition (Table 2), which on the basis of the available data may be regarded as marker of this Albano unit. Further distinctive chemical characters may be noted for the pumices of the basal layer of the unit ***d*** (layer ***d*–0**) which show the highest SiO_2, Al_2O_3, SrO and F contents and lowest MgO concentrations of the whole Albano series (Table 2) (cf. Table 2 of Freda et al., 2006a).

Particular important for the purpose of the present study, are also the recent petrological and geochemical investigations of the Colli Albani volcanological record (Gaeta et al., 2006), which point out a significant time dependance of the $^{87}Sr/^{86}Sr$ ratio. This isotopic ratio shows in fact a continuous decrease during the 600–36 ka time interval from the values of c. 0.7112, typical of the oldest products of the Tuscolano-Artemisio phase, to c. 0.70967–0.70941 or even less, typical of the most recent products of the Albano Maar (see Table 4 below). This isotopic ratio thus represents a further useful geochemical marker for the recognition of the Albano deposits even at great distance from the vent, where the alteration of the glass and the lacking of the typical stratigraphic structure may often make problematic the identification of the products.

Table 2
Electron microprobe analyses of interstitial glasses in juvenile clasts from the base of the proximal units ***d*** and ***f*** (location of the sampled sites in Fig. 1)

	Unit *f*-1						Unit *d*	
	Grey scoria Site 11		Yellow scoria Site 9				White pumice Site 16	
			a		b			
	n = 13	s.d.	*n* = 6	s.d.	*n* = 2	s.d.	*n* = 3	s.d.
SiO_2	47.01	0.85	46.42	1.15	43.09	0.31	49.68	1.18
TiO_2	0.54	0.05	0.59	0.10	0.94	0.06	0.12	0.03
$Al2O_3$	20.43	0.35	19.62	0.67	17.23	0.16	21.51	0.04
FeO	5.35	0.50	5.41	0.51	9.27	0.07	3.43	0.12
MnO	0.26	0.05	0.22	0.04	0.28	0.08	0.27	0.04
MgO	0.97	0.15	1.17	0.18	3.01	0.05	0.35	0.03
CaO	7.29	0.93	7.45	0.89	11.29	0.27	4.29	0.07
Na_2O	6.83	1.12	5.55	0.61	4.46	0.02	4.19	0.23
K_2O	6.35	1.52	7.54	1.58	5.36	0.03	8.66	0.37
BaO	0.15	0.15	0.23	0.04	0.23	0.04	0.23	0.05
SrO	0.37	0.46	0.25	0.12	0.20	0.04	0.47	0.07
P_2O_5	0.19	0.04	0.24	0.09	0.60	0.01	0.02	0.00
F	0.61	0.35	0.69	0.08	0.43	0.06	1.31	0.05
SO_3	0.38	0.07	0.43	0.04	0.33	0.03	0.23	0.02
Total	96.73		95.81		96.72		94.76	

n: number of analyses.
s.d.: standard deviation.

3. Mid-distal deposits and correlation with their proximal equivalents

3.1. Colli Albani area

3.1.1. General background

Field investigations allowed the recognition and the characterization of a succession of four pyroclastic deposits, here neutrally termed "distal unit 1–4" (DU1, DU2, DU3 and DU4), widely spread in the northeastern sectors of the Colli Albani volcano, within and beyond the Tuscolano-Artemisio caldera rim, as far as 15 km eastward from Albano Maar (Fig. 1). All units comprise pyroclastic fall deposits and possibly primary and reworked pyroclastic current deposits.

A basic description of the DUs, and the related proposed correlation with the proximal units, is reported in Fig. 3. In the following sections, we present and discuss the field data drawing attention to the importance of the above described Albano Maar markers (Section 2.3) as reliable tools to trace the correlations from proximal to mid-distal areas (2–15 km eastward from the crater) and possibly until a distance exceeding 100–120 km from the vent. Further morphological, pedostratigraphic, and archaeological data, corroborating the tephrostratigraphic-based correlation, are reported. The below proposed correlation is discussed both in the light of the original data presented in this study and in the broader context of the previous knowledge.

3.1.2. Internal sequence and components of the distal units

DU4—It is the uppermost and the most widespread unit, as testified by a number of the investigated stratigraphic occurrences (Fig. 4). Its internal sequence shows three well distinguished levels or subunits (Fig. 3). The basal subunit DU4a is a thin layer of yellowish, quite vesicular and moderately porphiritic pumice including outsized, very porphiritic greenish scoria with (up to mm-sized) leucite, dark mica and clinopyroxene crystals. Its thickness range from about 8–9 cm, within the Campi di Annibale area, to 3–4 cm or less at the most distal sections, with maximum diameter of the out-sized scoria of c. 4 cm and less than 1 cm, respectively. The DU4a layer is capped by a stratified ash deposit with mm- to cm-sized rounded scoria and accretionary lapilli (DU4b). At Campi di Annibale the DU4b reaches its maximum thickness of about 120 cm and shows a low-angle cross stratification, much more marked than at the other sections, where it tends to assume a plane-parallel lamination. However, the thickness of this subunit is sizeable in the whole dispersion area, even at very distal sections with minimum values of about 25–30 cm (Fig. 5).

Please cite this article as: Giaccio, B., et al., Mid-distal occurrences of the Albano Maar pyroclastic deposits and their relevance for reassessing the eruptive scenarios of the most recent activity at the.... Quaternary International (2006), doi:10.1016/j.quaint.2006.10.013

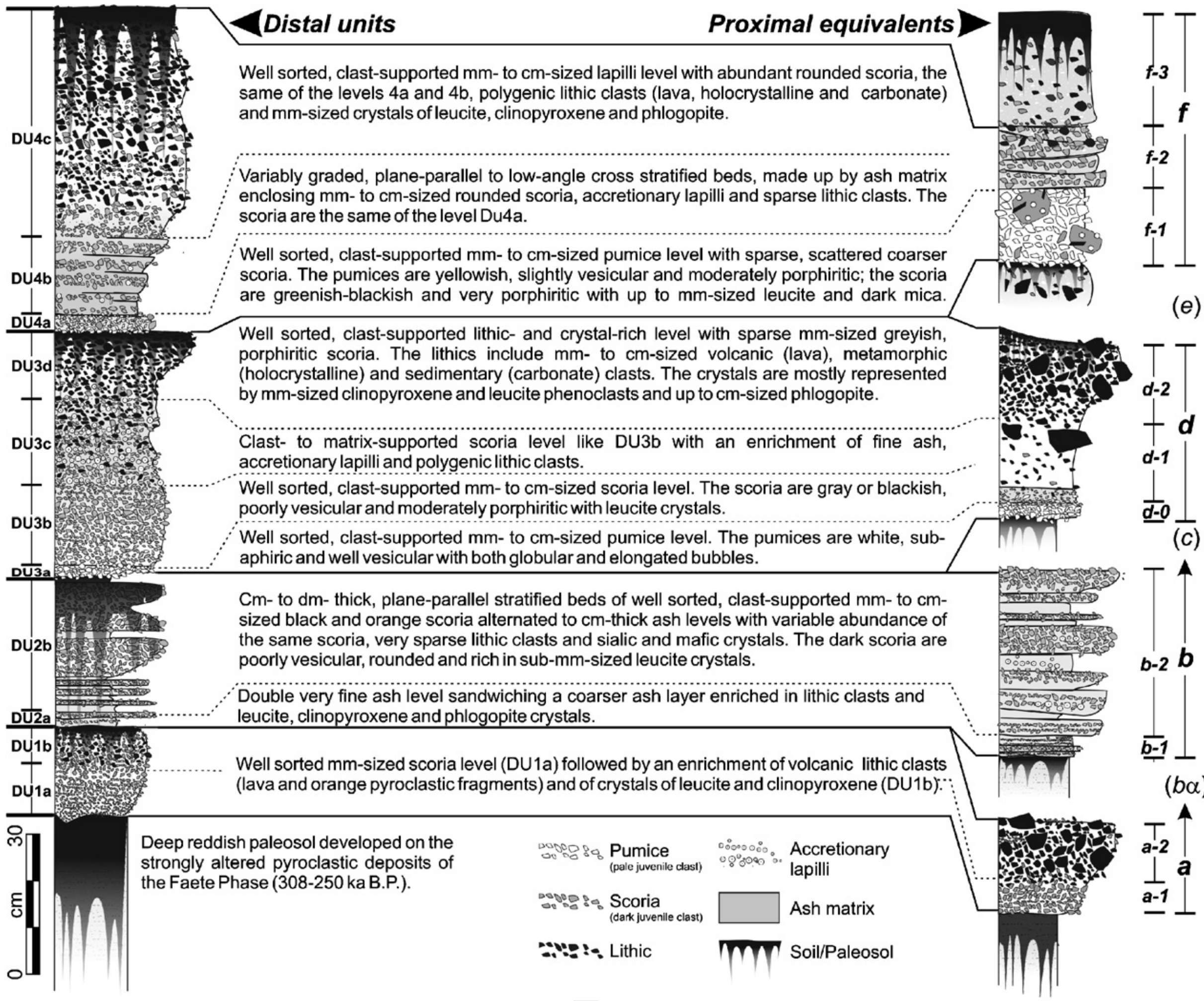

Fig. 3. Stratigraphic succession and description of the Albano distal units at most complete sections exposed near S. Cesareo Village (site n. 1 in Fig. 1), correlated to their proximal equivalents (stratigraphic logs of the proximal units not in scale).

The DU4b is followed by layer DU4c, which is a well sorted, clast-supported and slightly reversely graded deposit made up by rounded gray-green scoria, volcanic, metamorphic and sedimentary lithic clasts (lava, holocrystalline and carbonate) and (up to mm-sized) crystals of leucite, black and green clinopyroxene and dark mica.

Both the yellowish pumice of the DU4a and the greenish porphiritic scoria occurring in all the subunits are very distinctive components, equivalent, in their overall characters, to the juvenile clasts of the basal fall and/or the surge deposits of the proximal unit ***f***, to which may be hence confidentially correlated.

DU3—This unit, subdivided in four subunits (Fig. 3), shows at its base a thin layer (DU3a) made up by well sorted and well vesicular, sub-aphiric, white pumices. It is overlain by a well sorted, clast-supported mm- to cm-sized scoria level (DU3b) followed by a gradual enrichment of fine ash, accretionary lapilli, crystals and lithic clasts (DU3c). Upward, while the amount of ash and accretionary lapilli decreases abruptly, the lithic and crystal abundances increase progressively, these components becoming predominant in the uppermost level DU3d (see Fig. 3 for further details).

The white pumice layer DU3a is virtually identical to those recognised at the base of the proximal unit ***d***. In addition, both the uppermost part of the DU3 and of the unit ***d*** are characterised by a well sorted and compositionally comparable lithic- and crystal-rich layer (subunit DU3d and ***d*-2**, respectively). The concurrence of both these distinctive marker layers in the same stratigraphic position of the respective internal sequences, strongly supports the correlation between the distal DU3 and proximal unit ***d***. Transitively, this very confident attribution makes the DU3 a reliable stratigraphic marker, leading and corroborating the correlation of the overlying DU4, as well as of the underlying DU2 and DU1 with their respective proximal equivalents.

DU2—This unit has at its base a peculiar double layer of fine ash sandwiching a coarser ash level (DU2a), followed by cm- to dm- thick, plane-parallel stratified beds of well sorted, clast-supported mm- to cm-sized black and orange scoria alternated to cm-thick ash levels with variable abundance of the same scoria (DU2b; Fig. 3). The poorly

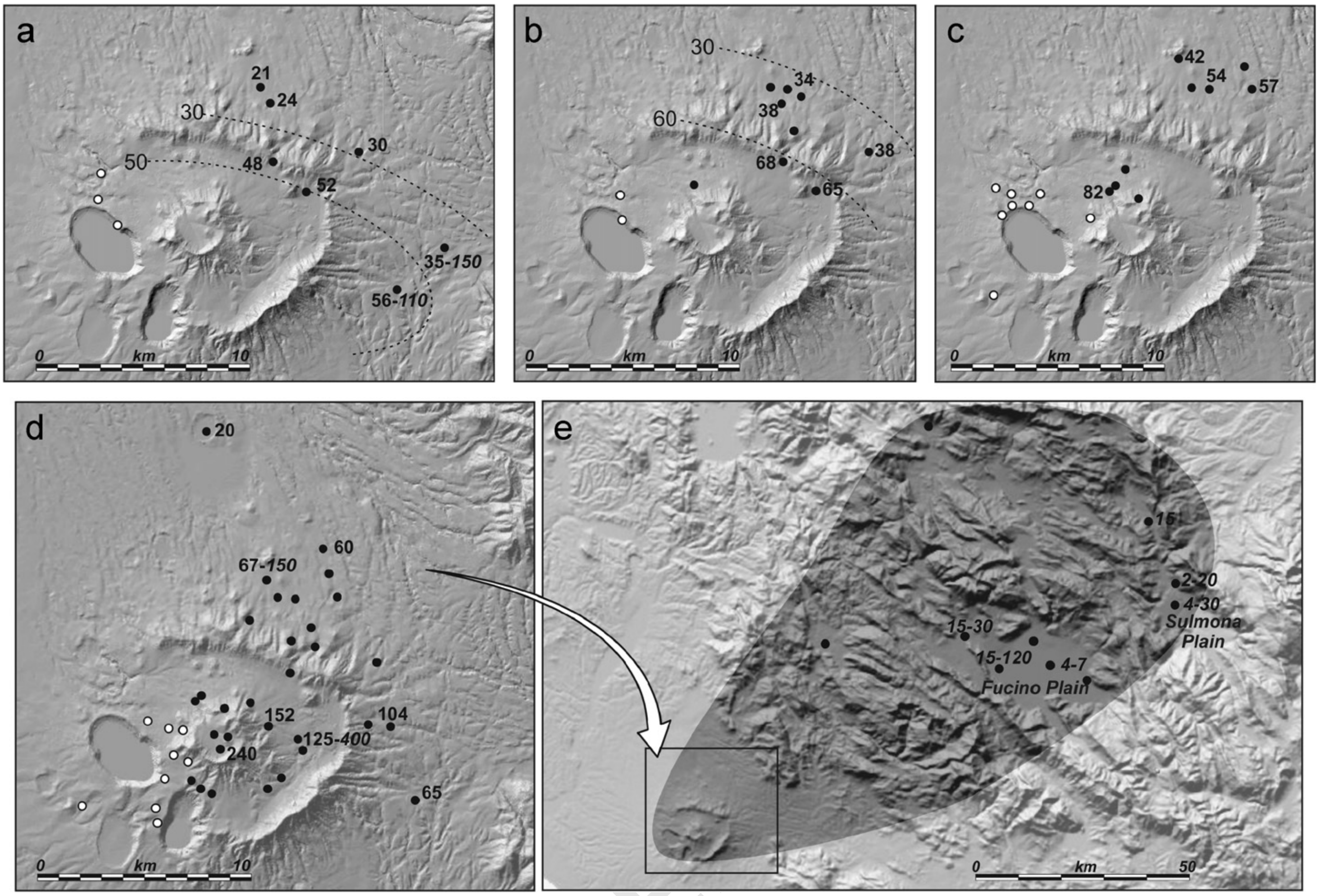

Fig. 4. Distribution of the four distal units (DUs) (black dots) and of the equivalent investigated proximal deposits (white dots): (a) DU1 with inferred isopachs (in cm); (b) DU2; c) DU3; (d) DU4; (e) Central Apennine occurrences of ash layer(s) correlated to the Albano Maar pyroclastic deposits (see Section 3.2. for details). The numbers indicate the deposit thickness in cm; in italic if reworked.

vesiculated and sub-rounded black scoria clasts contain adbundant sub-mm-sized leucite crystals. Both the internal sequence and the character as a whole of the components of DU2, including the internal texture of the black scoria, show strong analogies with the proximal unit ***b***. In particular, layer DU2a may be confidentially equated to ***b*–1**, while DU2b would comprise layer ***b*–2** and possibly some more layers of unit ***b*** of fallout origin (***b*–3**, **4**, **11**, **12**, and **13**).

DU1—The lowermost distal unit is a well sorted, faintly graded, clast-supported aggregate of mm- to cm-sized, poorly vesicular and moderately porphiritic, black and brown scoria containing up to mm-sized clinopyroxene, leucite and olivine crystals. It has been divided in two subunits, the lower one made up almost exclusively by juvenile clasts (DU1a), the upper one enriched in lithic clasts and crystals (DU1b). The lithics are predominantly of volcanic origin and comprise lava and peculiar strongly altered, red-orange pyroclastic fragments.

The lowermost DU1 can be confidentially correlated to the earliest Albano proximal unit ***a***, because (i) the juvenile clasts of DU1, although hardly idiosyncratic in terms of textural features, my be equated to those of the proximal unit ***a*** for the appreciable presence of olivine crystals; (ii) DU1 occurs systematically in strict stratigraphic relationship with the other Albano distal units, with which it forms a discrete, concordant depositional sequence; (iii) unit DU1 is almost always directly overlain by unit DU2 and is separated from the latter only by a poorly developed brown PS, suggesting a relatively short time interval between deposition of these two units.

Reworked deposits—with the exception of the DU3, distal units, and particularly DU4, may locally be buried, or even completely replaced, by thick deposits deriving from the reworking of the primary pyroclastic units (Fig. 5). These reworked deposits are generally much thicker than primary ones, and are systematically associated to morphological depressions, such as the semi-closed basins of the Tuscolano-Artemisio and Campi di Annibale calderas and/or some of the main drainage valleys along the north-eastern slope of the Tuscolano-Artemisio.

The contact with the underlying, undisturbed deposits may be either paraconcordant or strongly discordant, with deep unconformity surfaces often involving the whole thickness of the primary deposits. Reworked deposits show variable lithofacies and sedimentary structures comprising,

Please cite this article as: Giaccio, B., et al., Mid-distal occurrences of the Albano Maar pyroclastic deposits and their relevance for reassessing the eruptive scenarios of the most recent activity at the.... Quaternary International (2006), doi:10.1016/j.quaint.2006.10.013

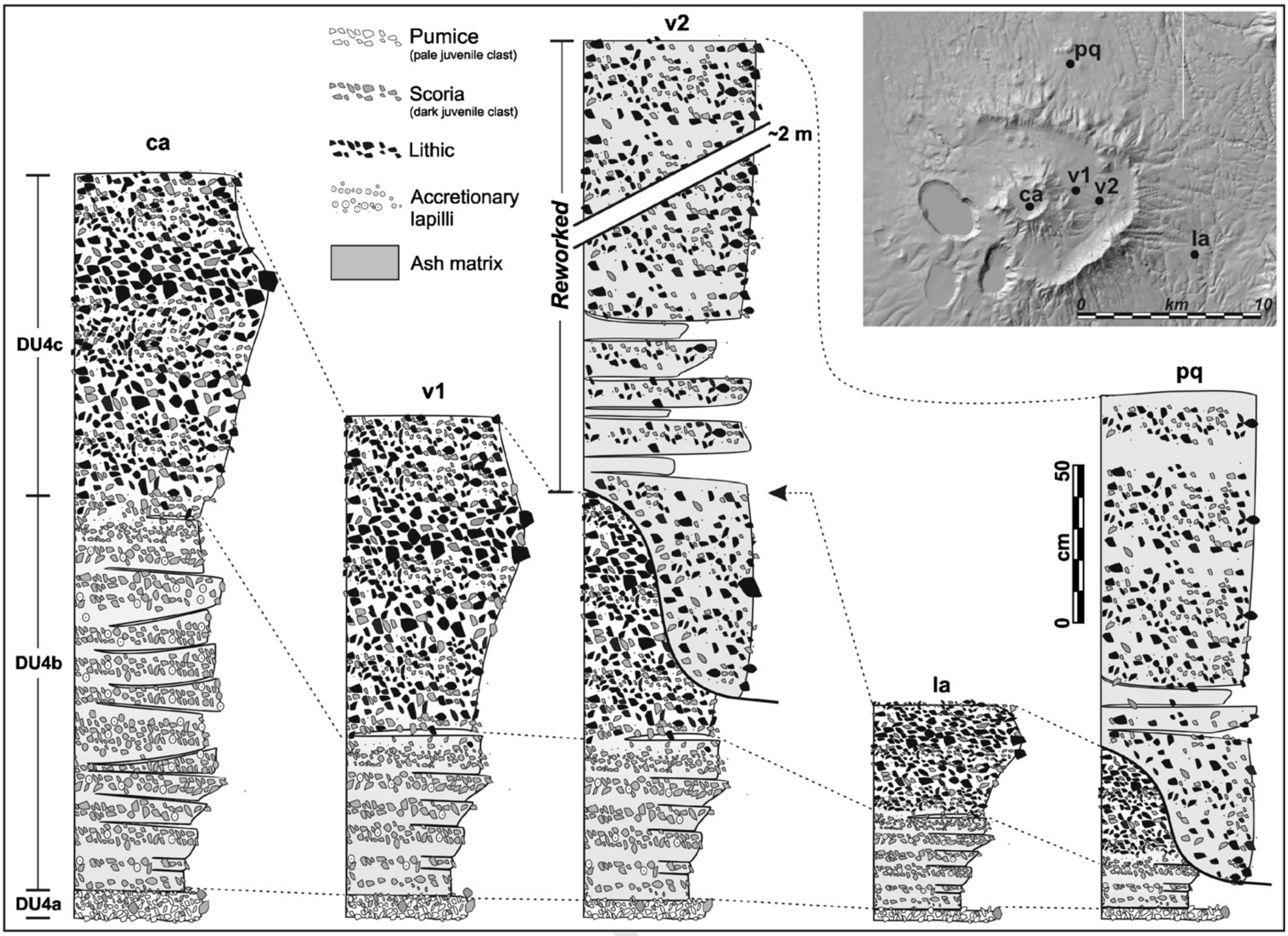

Fig. 5. Representative stratigraphic logs of the Albano distal unit 4 (DU4).

principally, massive, matrix-supported ash and lapilli beds; fines-poor depleted high-angle cross stratified ash and lapilli and thinly stratified, plane-parallel ash deposits. This wide spectrum of lithofacies suggests different secondary transport and deposition mechanisms, possibly including both catastrophic, syneruptive mud/debris flows (lahars) and ordinary fluvial/lacustrine sedimentary processes. In this regard, of note is the case of the caldera depression of the Tuscolano-Artemisio, where we identified a system of lacustrine terraces and related deposits, whose formation appears to be closely linked to the primary deposition and reworking of the distal units. However, space prevents us for an extensive treatment of this subject, which we intend to deal with in a near future elsewhere.

3.1.3. Petrological and geochemical data

Microtextural and compositional features—Several sampled pyroclastics resulted too weathered and thus unsuitable for thin sections and microprobe analyses (for detail on analytic methods see Appendix A). For this purpose, we selected relatively fresh samples of the DU4a, DU3a, DU3b and DU2 units from the sites 1 (S. Cesareo), 2 (Campi di Annibale) and 8 (Castiglione lacustrine core) (location sites in Fig. 1). Additional observations on the textural characters and mineralogical compositions were carried out on the loose deposits of several samples of all the DUs.

DU4a—Millimetre-scale dark scoria and yellowish pumice clasts are the most abundant component in the DU4a subunit. The former are porphyritic, poorly vesicular and characterised by cryptocrystalline zeolitised groundmass, while the latter are sub-aphiric and more vesicular. Phenocrysts of the darker juvenile clasts include clinopyroxene, leucite, nefeline, sanidine, phlogopite, garnet, amphibole, hauyna and accessory minerals. Small zones of light-brown glass are rarely present on the clinopyroxene rims. Common phenoclasts of main phases (clinopyroxene and leucite), scarce volcanic lithic clasts and rare leucite-bearing glassy scoria clasts are also present in these rocks. Glasses compositions measured by electron microprobe are K-foiditic (Fig. 6) and show a high Na_2O content (Table 3). Clinopyroxenes are predominant in both the juvenile scoria clasts and the matrix. They are millimetre-scale, subhedral to euhedral, pleochroic (green to light brown) with

Please cite this article as: Giaccio, B., et al., Mid-distal occurrences of the Albano Maar pyroclastic deposits and their relevance for reassessing the eruptive scenarios of the most recent activity at the.... Quaternary International (2006), doi:10.1016/j.quaint.2006.10.013

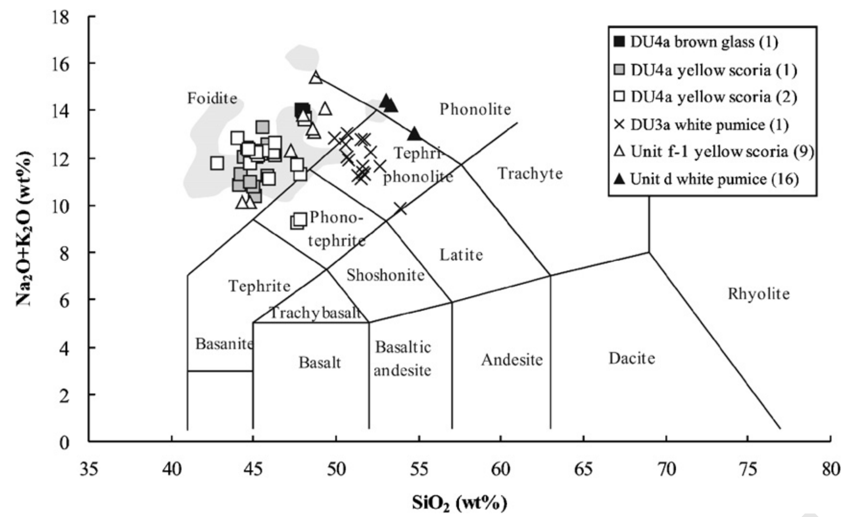

Fig. 6. Chemical composition of interstitial glasses from juvenile clasts of the DU3a, DU4a and proximal units ***d*** and ***f*** (Tables 2 and 3) plotted on the total alkali silica diagram. The field of the chemical composition of the interstitial glasses from juvenile clasts of the Albano Maar products reported in Freda et al. (2006a) is also shown (grey area). Numbers in parentheses refer to the sampled site (location in Fig. 1).

Table 3
Electron microprobe analyses of interstitial glasses from juvenile clasts of the DU3 and DU4 (location of the sampled sites in Fig. 1)

	DU4		DU4a						DU3a	
	Grey scoria		Brown glass		Yellow scoria				White pumice	
	Site 8		Site 1		Site 1		Site 2		Site 1	
	n = 2	*s.d.*	*n* = 3	*s.d.*	*n* = 16	*s.d.*	*n* = 12	*s.d.*	*n* = 15	*s.d.*
SiO_2	42.89	0.93	45.38	0.38	44.19	1.71	43.27	0.71	49.18	1.08
TiO_2	0.84	0.09	0.74	0.03	0.84	0.09	0.80	0.12	0.36	0.05
Al_2O_3	18.32	0.53	18.86	0.25	18.18	0.73	18.69	0.51	21.13	0.58
FeO	7.87	0.33	6.19	0.15	8.14	0.79	7.86	0.75	6.22	0.38
MnO	0.33	0.01	0.23	0.06	0.30	0.08	0.30	0.04	0.45	0.06
MgO	1.24	0.05	1.06	0.09	1.33	0.49	1.16	0.22	0.60	0.06
CaO	11.66	0.32	8.78	0.12	10.66	1.09	11.09	1.00	6.12	0.57
Na_2O	6.18	0.49	4.28	0.05	5.11	1.04	5.57	0.56	5.25	0.66
K_2O	5.26	0.01	8.85	0.19	6.25	1.37	5.62	1.09	6.12	0.73
BaO	nd	nd	0.15	0.02	0.10	0.05	0.09	0.04	0.21	0.05
SrO	nd	nd	0.13	0.03	0.29	0.18	0.28	0.12	0.75	0.11
P_2O_5	0.30	0.01	0.12	0.03	nd	nd	nd	nd	0.09	0.03
F	0.73	0.05	0.42	0.14	nd	nd	nd	nd	1.41	0.24
SO_3	1.01	0.04	0.60	0.06	0.74	0.38	1.19	0.40	0.30	0.22
Total	96.63		95.79		96.13		95.92		98.19	

n: number of analyses.
s.d.: standard deviation.

inclusions (glass, apatite, magnetite, and phlogopite), and frequent garnet and leucite intergrowths. Subhedral, light green clinopyroxenes with pitted surfaces are also present. Clinopyroxene compositions obtained by microprobe analyses are characterised by an enrichment in Fe, Al and Ti and depletion in Si contents. Microtextural features, Na_2O-rich glasses and clinopyroxene mineral-chemistry of DU4a scoria clasts are similar to those reported in this study and by Freda et al. (2006a) for the juvenile components present in the unit ***f***.

DU3—The white pumices of the subunit DU3a are well vesicular and show a less porphyritic microtexture characterised by a lower mafic vs. sialic minerals ratio respect to the juvenile components of DU4a, with sparse phenocrysts of deep green clinopyroxene, leucite and nefeline. The groundmass is characterised by colourless glass and abundant cryptocrystalline leucite. Both clinopyroxene phenocrysts and stretched bubbles show a preferential orientation of the elongate axis. The main difference moving in the subunit DU3b is the decreasing of the glass amount and vesiculation degree. The glasses from DU3a plot in the tephri-phonolite field of the total alkali-silica diagram (Fig. 6) and are characterised by high SiO_2, Al_2O_3 and Na_2O contents (Table 3). The glass compositions and the microtextural features of DU3a are comparable with those of the white pumices present at base of the proximal unit ***d*** of the Albano maar described by Freda et al. (2006a) and analysed in the present study (Table 2). In particular, although a certain difference may be noted, the pumices of the DU3a show the same high SiO_2, Al_2O_3, SrO and F contents characterising the colourless glass of the unit ***d*** (Tables 2 and 3). Preliminary petrologic calculations suggest that the slight chemical differences between DU3a and proximal unit ***d*** glasses are consistent with a more differentiated composition of DU3a glasses as pointed out by their higher Na_2O content and lower K_2O/Na_2O ratio. Moreover, these glasses have different volatile contents as shown by the total values of chemical analyses reported in Tables 2 and 3 (volatiles = 100−total).

DU2—In thin section, the DU2 is distinguishable respect to the overlying units by the scarcity of millimetre-scale leucite phenoclasts. In particular, the poorly vesicular scoria clasts show abundant micro-phenocrysts ($<200\,\mu m$) of leucite coupled with rare millimetre-scale, colourless to green, subhedral to euhedral clinopyroxenes. The sampled DU2 juvenile clasts resulted too altered for microprobe analyses; however their microtexural features correspond to those reported by Freda et al. (2006a) for the juvenile components in the proximal unit ***b*** of the Albano maar.

DU1—Its most distinctive character is a significant abundance of olivine crystals, which are virtually absent in the other DUs. Significantly, according to Freda et al. (2006a), within the proximal stratigraphic suite of the Albano Maar, olivine crystals occurs only in some layers of the earliest unit ***a***.

In conclusion, all the above-reported data and observations indeed support the proposed tephrostratigraphic correlation (Fig. 3).

$^{87}Sr/^{86}Sr$ ratio—In order to obtain additional geochemical constraints on the studied deposits, as well as to test their consistency with the lithostratigraphic correlation, we performed strontium isotopic analyses on clinopyroxenes from all distal units, as well as from some layers of the Albano proximal deposits (details on analytic methods in Appendix A). The $^{87}Sr/^{86}Sr$ ratio measured on the DUs clinopyroxenes ranges from 0.70963 to 0.70945, i.e. the same discrete interval characterising the pyroclastic products of the Albano Maar (Table 4). Indeed, on the basis of the available data, any alternative correlation would be inconsistent with the determined isotopic ratio. In this regard, the values of the $^{87}Sr/^{86}Sr$ ratio related to the distal subunit 4a (DU4a) and proximal ***f*−1/2**, both comprise within the same narrow interval between 0.70958 and 0.70953, are particularly convincing.

3.1.4. Additional chronological clues corroborating the correlation

Morpho-pedostratigraphic context—Throughout their dispersion area, the distal units overlie a reddish PS developed on peri- and intra-caldera eruptive products of the Faete Phase (308–250 ka). The PS, here termed Faete PS, is several metres deep and shows strong alteration of the parent material indicating significant exposure, possibly encompassing one or more glacial/interglacial climatic cycles. By comparison, the three PSs separating the four units—PS1, PS2 and PS3, affecting the top of DU1, DU2 and DU3, respectively—are generally brown and shallow, both features suggesting a shorter exposure time as well as colder and more arid climatic conditions, consistent with those of the Last Glacial period (c. 70–11.5 ka B.P.). Moreover, within the same dispersion area, the depositional top of the distal units almost always coincides with the present topographic surface, with the volcaniclastic succession mantling the paleo-landscape of relatively mature and deep drainage networks. These pedostratigraphic and geomorphic features indicate not only that the deposition of the distal units was quite recent, but also that their emplacement was preceded by a sufficiently long period of quiescence in the volcanic activity for the development of the deep Faete PS and a mature hydrographic network. The above considerations bear geochronological clues supporting again the correlation of the distal units with the most recent activity of Colli Albani, i.e., that of the Albano Maar.

Furthermore, the deepest and more evolved PS occurring within the distal succession is the PS2, separating the products of DU2 from those of DU3, i.e. the PS which, according to the proposed correlation (DU2 = ***b***; DU3 = ***d***), should coincide with the main temporal hiatus documented within the geological record of the Albano Maar by Ar/Ar chronology, separating the Early (70–68 ka) from the Late (41–36 ka) eruptive cycle (Fig. 3; Table 1). On the contrary, the relatively less evolved and shallow PSs PS1 and PS3 indeed indicate shorter DU1-2 and DU3-4 inter-eruptive time intervals. As a whole, the internal pedostratigraphic features indicate appreciable differences in terms of timing of the inter-eruptive intervals consistent with the $^{40}Ar/^{39}Ar$ chronology of the proximal Albano Maar deposits (Table 1).

Archaeological context—Systematic surveys and previous archaeological research allow to recognise and map several dozens of open-air, Middle Palaeolithic sites in the Colli Albani area (Fig. 7). All sites show lithic assemblages with homogeneous typological and technological characters that belong to the so-called Pontinian Mousterian, a regional variant of the Mousterian technocomplex characterised by an industry made on small flint pebbles (for further details about the artefact typology see Rolfo et al., in press and reference therein). At stratified cave sites, the Pontinian Mousterian is dated between c. 100 and 32 ka B.P., with the bulk of the available dates falling within the

Table 4
$^{87}Sr/^{86}S$ analyses of clinopyroxene crystals of the investigated distal units (DUs) compared with similar known values for the Albano Maar proximal units and some eruptive units representative of the three main phases of the Colli Albani Volcanic District

Site	Sample	Phase	Unit	Age (ka)	87Sr/86Sr	$\pm 2\sigma$
A3	CES-2		Distal tephra	45–30	0.70969	2×10^{-5}
2	CA-A4c	LH[a]	DU4c	LG[b]	0.70958	2×10^{-5}
	CA-A4a		DU4a		0.70957	2×10^{-5}
1	S-A4c		DU4c		0.70953	2×10^{-5}
	S-A4a		DU4a		0.70953	2×10^{-5}
	S-A3d		DU3d		0.70959	2×10^{-5}
	S-A3c		DU3c		0.70963	2×10^{-5}
	S-A2b		DU2b		0.70963	2×10^{-5}
3	B-A3d		DU3d		0.70955	2×10^{-5}
5	L-A1		DU1		0.70950	2×10^{-5}
8	CAS		DU4c	36–35[c]	0.70945	2×10^{-5}
9	SCI-f	LH	AL(***f**-1/2*)	36	0.70953	2×10^{-5}
10	PC-d2		AL(***d**-2*)	41–36	0.70967	2×10^{-5}
14	AH-17, 1*		AL(***f**-1/2*)	36	0.709544	1×10^{-5}
	AH-3C16/4Fb*		AL(***f**-1/2*)	36	0.709579	1×10^{-5}
Albano Lake (12)	AH-3A, 5*		AL(***a**-1*)	69	0.708508	1×10^{-5}
	AH-3A, 4*		AL(***a**-1*)	69	0.709416	0.9×10^{-5}
15	AH-9, 5*		AL	41	0.709621	0.9×10^{-5}
	AH-9, 4*		AL	41	0.709675	0.9×10^{-5}
	AH-1D*		AR	204	0.710109	1.3×10^{-5}
4	CAR-F	F	PSC	–	0.71031	2×10^{-5}
13	AH-7A*		MM	308	0.710304	0.9×10^{-5}
	AH-7*		MM	308	0.710382	0.9×10^{-5}
	UFU*	T-A	VS	366	0.710506	1×10^{-5}
	PN*		PN	407	0.710543	0.9×10^{-5}
	PR*		PR	457	0.710654	0.9×10^{-5}
	T*		LV	460	0.710643	1.4×10^{-5}
	TP*		TP	528	0.710893	0.9×10^{-5}
	P*		TTC	561	0.711069	1×10^{-5}
	C4*		CA	608	0.711200	0.9×10^{-5}

A significant consistence between the values of the DUs and the Albano Maar deposits can be noted.
*Data from Gaeta et al. (2006).
Abbreviations: LG: Last Glacial period; LH: Late Hydromagmatic; F: Faete; T-A: Tuscolano-Artemisio; AL: Albano Maar (in brackets related units/subunits); AR: Ariccia Maar; PSC: Peri-caldera scoria cone; MM: Mt. Mellone lava flow; VS: Villa Senni Eruptive Unit; PN: ozzolane nere; PR: Pozzolane Rosse; LV: Vallerano lava flow; TP: Tufo del Palatino; TTC: Trigoria-Tor de' Cenci Tuff; CA: Cave fall layer.
[a]According to the tephrostratigraphic correlation (see Section 3.1.2 for details).
[b]Inferred from morpho-pedostratigraphic and archaeological setting (see Section 3.1.4 for details).
[c]According to the age model for the Castiglione lacustrine pollen record (Follieri et al., 1988).

shorter temporal interval of 80–45 ka (Khun, 1995 and references therein).

In all the investigated sites, the lithic industry has been systematically found in the uppermost horizon of the deep PS developed on the final pyroclastic deposits of the Faete Phase (Faete PS); i.e. the same pedomarker underlying the sequence of the four DUs. Unfortunately, a large amount of the sites are sub-superficial and non stratified, with the Faete PS almost coinciding with present topography or barely eroded. In this regard, are particularly important the recent archaeological investigations near Colonna village, where the Faete PS containing some Pontinian artefacts is directly buried by a sequence comprising DU3 and reworked DU4.

By considering the available chronology of both Colli Albani Volcanic District and Pontinian Mousterian industry, such a pedo-tephrostratigraphic context of the archaeological findings, not only supports the proposed correlation of the distal units to the Albano Maar, but also would rule out any possible alternative attribution. Indeed, on the basis of the available chronological data (e.g. Marra et al., 2004), within the whole geological record of the Colli Albani Volcanic District, only the Albano Maar products have an age consistent with the Pontinian Mousterian industry.

Noteworthy, the spatial distribution of the Pontinian open-air sites shows numerous occurrences along the southern and north-western piedmont zone of the Tuscolano-Artemisio and a complete absence of archaeological traces on the north-eastern slope (Fig. 7). Although this pattern may represent an actual archaeological, palaeoecological datum indicating a precise strategy of the human settlements, the surprising negative correlation between Pontinian site density and distal unit distribution would suggest a purely geological, non-cultural cause. In fact, contrary to the southern and north-western areas, where

Please cite this article as: Giaccio, B., et al., Mid-distal occurrences of the Albano Maar pyroclastic deposits and their relevance for reassessing the eruptive scenarios of the most recent activity at the.... Quaternary International (2006), doi:10.1016/j.quaint.2006.10.013

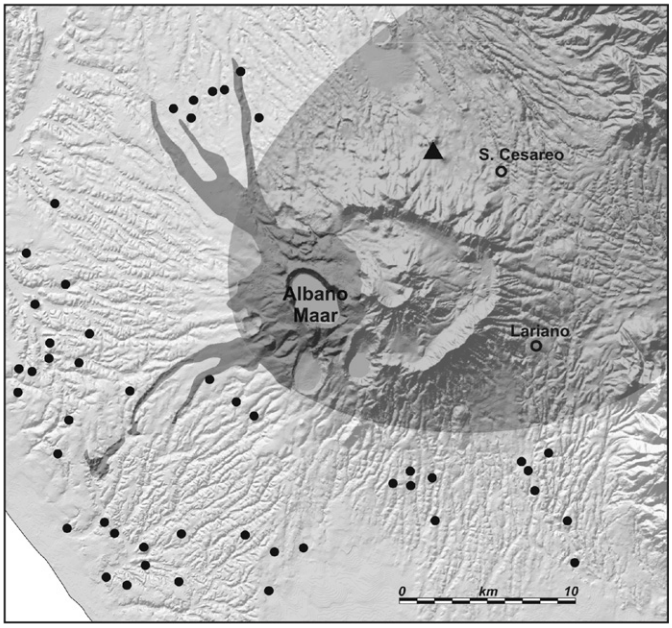

Fig. 7. Distribution of the Mousterian Pontinian sites within the Colli Albani area (see also Rolfo et al., in press) and its relationship with the inferred areal dispersion of the Albano Maar pyroclastic flow (darker shadowed area) and fall (lighter elliptical shadowed area) deposits. Black dots: sub-superficial Pontinian open-air sites; black triangle: Pontinian site buried by the Albano distal unit 3 (DU3) (see Section 3.1.4. for details).

the Faete PS containing the Pontinian industry is widely outcropping, in the north-eastern sector of the Tuscolano-Artemisio this pedo-archaeological horizon, may be obliterated by the pyroclastic deposits of one or more distal units, as testified by the Colonna stratified site. The consequent reduced archaeological visibility is hence a possible concurrent cause of the observed marked difference in density of the Pontinian sites.

Occurrence and age of the DU4 in the Castiglione lacustrine record—The Castiglione lacustrine sequence hosts one of the longest and continuous pollen record of the central Mediterranean area, documenting the climatic history of the last 250,000 years (Follieri et al., 1988). Its chronology is based on several combined and very concordant dating methods comprising 21 radiocarbon measurements, correlation of the main, well documented climatic oscillations with marine oxygen isotope record and counting annual lamination layers (Follieri et al., 1988). All these independent methods gave a constant sedimentation rate of about 0.31–0.32 mm/year from the base to the top of the core.

In addition to the deposits outcropping in a number of natural sections (Fig. 1), we examined a relative coarse and thick tephra layer (c. 20 cm) occurring in the sediment core of the Castiglione Maar lacustrine sequence (sample courtesy of prof. D. Magri) between 11.40 and 11.20 m depth. Our componentry, textural and chemical analyses of this ash layer indeed indicates strong analogies with the DU4, more precisely with the uppermost and widespread subunit DU4c. In particular, the chemical composition of the juvenile clasts of the Castiglione layer, with very high Na_2O content, is virtually the same of the DU4 and its proxilmal equivalent unit ***f*** (Tables 2 and 3). A $^{87}Sr/^{86}Sr$ ratio measurement on clinopyroxene crystals from this layer also confirms its broad correlation to the Albano products (Table 4). According to the above age model, the ash layer equated to the DU4 should be dated between 36,500 and 35,400 ka B.P., i.e. the same age of the Albano Maar unit to which has been lithostratigraphically and chemically independently correlated.

3.2. Central Apennine area

3.2.1. Stratigraphical, chronological and geochemical data

Field investigations in the central Apennine intermountain basins of Fucino, Sulmona, Tirino and Aterno valley enable us to recognise several sections of Late Pleistocene fluvio-lacustrine and alluvial deposits containing one or more cm- to dm-thick crystal-rich reworked tephra layers (Figs. 4e and 8). These are made of sub-mm- to mm-sized poorly vesicular grey-black scoria with abundant clinopiroxene, leucite and up to cm-sized phlogopite crystals.

In the Sulmona Plain (Fig. 8, site A1), one of these crystal-rich tephra layers occurs within deposits of a braided fluvial system its depositional top surface defining a wide and well preserved terrace known as the "Terrazza Alta di Sulmona"(e.g. Demangeot, 1965; Miccadei et al., 1999). A radiocarbon measurement performed on terrestrial gasteropod shells embedded in this ash yielded an age of 31,585 ± 210 ^{14}C years B.P., roughly corresponding to an age of 36,610 ± 209 cal years B.P. (estimate calibration according to Fairbanks et al., 2005), i.e. an age statistically indistinguishable from those of the most recent eruption of the Albano Maar (Table 1).

In the Tirino Plain, a similar tephra layer occurs within lacustrine-alluvial deposits, dated between 41,990 ± 1550/34,680 ± 830 and 28,900 ± 600 ^{14}C years B.P., overlaying a PS containing Middle Palaeolithic-Mousterian artefacts associated with large mammal bones (Fig. 8, site A2).

Moreover, we performed a $^{87}Sr/^{86}Sr$ isotopic ratio measurement on clinopiroxene crystals of the uppermost level of two crystal-rich tephra layers occurring at the top of the Late Pleistocene fluvial-lacustrine deposits of the Fucino Plain outcropping near Avezzano (Fig. 8, site A3). This analysis yielded a value of 0,70969, comparable with those characterising the Albano units (Table 4).

On the grounds of our available ^{14}C dating, these tephra may be roughly dated between 45 and 30 cal ka B.P. Although during this time span several Campanian and Sicilian explosive volcanoes were active, the componentry of these layers and, in particular, their high content of leucite crystals, indicating a foiditic magma composition, allow us to reasonably exclude any possible volcanic source other than the Albano Maar. The most widespread tephra layers in central Mediterranean area, dated between 45 and 30 ka B.P., are in fact mostly trachytic/trachytic-phonolitic in composition and indeed do not contain the large amount

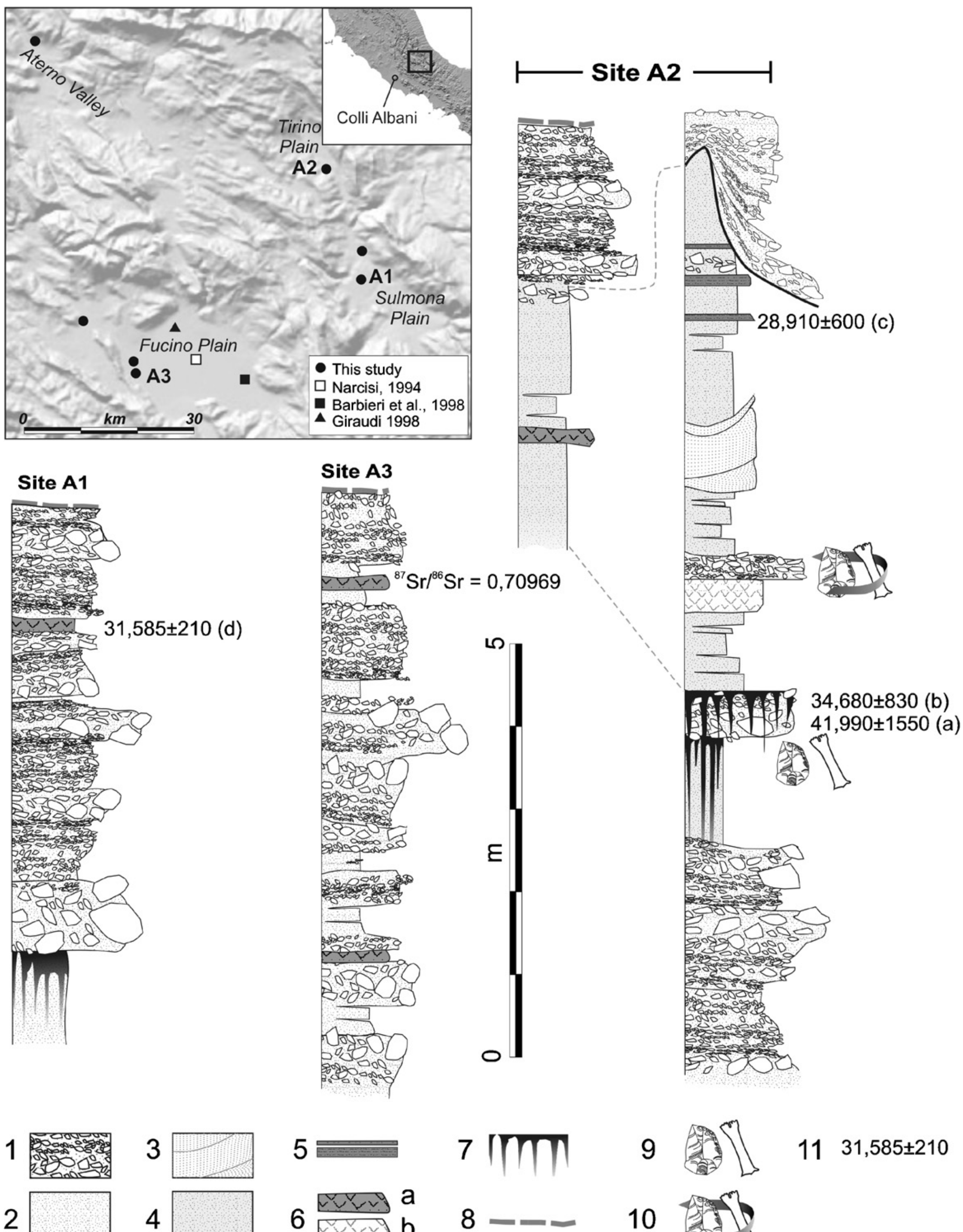

Fig. 8. Reference map and stratigraphic logs of some of the investigated Late Pleistocene sequences of the Central Apennine containing the crystal-rich tephra layers correlated to the Albano Maar products: (1) gravel, (2) sandy matrix; (3) cross-stratified sand; (4) silt; (5) peat levels; (6) tephra layer a—leucite-rich ash, b—trachytic ash; (7) paleosol; (8) well-preserved depositional top surface; (9) in situ Mousterian artefacts with large mammal bones; (10) Reworked artefacts with large mammal bones; (11) uncalibrated radiocarbon dating: a—on charcoal, b—on paleosol, c—on peat level, d—on terrestrial gasteropod shell.

of potassic feldspathoid characterising these central Apennine leucite-rich tephra layers (e.g. Paterne et al., 1988; Narcisi and Vezzoli, 1999; Wulf et al., 2004). This conclusion is further supported by the determined value of 0,70969 of the $^{87}Sr/^{86}Sr$ ratio. In fact, the products of all the Peninsular and Insular Italian volcanoes, active during the time span estimated for the deposition of these tephras, have a much lower $^{87}Sr/^{86}Sr$ ratio $<0,708$ (e.g. Ayuso et al., 1998; Barbieri et al., 1998; Pappalardo et al., 1999).

Unfortunately, the considerable thickness variability, from a minimum of some centimetres up to a metre or more, and the overall sedimentary structures clearly indicate a certain degree of post-depositional reworking of volcanic ash, which prevent us to estimate the actual thickness of the primary ash fall deposits. In spite of this, considering their significant diffusion, the value of 2 cm may be reasonably regarded as a minimum, very conservative thickness estimate.

3.2.2. Additional data from previous studies

Tephra layers showing the same peculiar componet features of those described in the above section, have been previously recognised in the Fucino lake sediments and in the surrounding alluvial and glacier Late Pleistocene depositional systems (e.g. Narcisi, 1994; Giraudi, 1998) and used as local tephrostratigraphic markers (Giraudi and Frezzotti, 1997). On the basis of their K-Foiditic chemical composition and age estimation, Narcisi (1994) attributed these ash layers to the most recent volcanic activity of the Colli Albani Volcanic District documented at the Albano Maar. More recently, a detailed chronological and geochemical isotopic study of four tephra layers, occurring within a fluvial/lacustrine sequence of the Fucino basin, definitely confirms their correlation to the Albano Maar deposits (Barbieri et al., 1998). More precisely, according to this study the four tephra layers have U/Th ages and $^{87}Sr/^{86}Sr$ ratios consistent with those of the four Albano Maar units of the Late eruptive cycle, i.e. the units ***c–f***.

Occurrence of seven tephra layers correlated to the Albano Maar activity are reported even in the Monticchio Lake sequence, Vulture volcano, southern Italy, at a distance exceeding 200 km south-east from the vent (Wulf et al., 2004). However, six of these layers, labelled TM-17a–TM-17f, contain a certain amount of plagioclase crystals, which instead are quite rare within the Colli Albani products, including the Albano Maar ones (e.g. Freda et al., 2006a). Furthermore, the recently acquired data on the chemical composition of Albano Maar, reported in this study and in Freda et al. (2006a), point out significant difference with those of the Monticchio tephras. In fact the latter generally show a lower alkali content (8–10%) and a higher silica concentration (48–53%) compared with the Albano Maar products (c. 10–15% and 40–50%, respectively; Fig. 7). Therefore, on the basis of the data available up to now, we are incline to regard this correlation as dubious.

4. Discussion

4.1. Previous different interpretation

In contrast with the above-proposed correlation, the pyroclastic deposits outcropping within the Tuscolano-Artemisio caldera, correspondig to the here labelled DUs, were previously mapped as products of a hydromagmatic centre located within the smaller caldera of the Campi di Annibale (De Rita et al., 1988), centred on the Faete stratovolcano (Fig. 1), the main magmatic activity of which has been recently dated between 260 and 250 ka B.P. (Marra et al., 2003). More recently, Giordano et al. (2006), in agreement with the present study, recognised the dispersion of these products beyond the Tuscolano-Artemisio caldera rim, even if they retained the previous interpretation of an origin in the Campi di Annibale area, as explicitly revealed by the term "Campi di Annibale phreatomagmatic succession" for these pyroclastics.

Independently from our above-reported data, which strongly support the correlation with the Albano Maar proximal products, several lines of evidence rise, in our opinion, significant doubts about the Giordano et al.'s interpretation.

Indeed, the Campi di Annibale area shows evidence of a post-caldera activity testified by a number of geomorphically well-preserved scoria cones, the slopes of which are locally mantled by the deposits of the DU4, attributed by De Rita et al. (1985) and Giordano et al. (2006) to a local hydromagmatic centre. However, in spite of this stratigraphic relationship, there is no geomorphological evidence of a hydromagmatic centre (maar or tuff ring) following the formation of the scoria cones. Another relevant point is that the deposits of the DU4, here widely exposed, do not show the typical proximal characters expected in a near vent setting, like the presence of large ballistic bloks, sharp grain size and facies variations, and rapid lateral thickness decay. Conversely, they are distributed almost uniformly and show homogeneous characters in the whole area of the Campi di Annibale, caldera similar to those occurring in more distal sections (Fig. 5), even in the central zone of the depression, where, according to the local origin hypothesis, the vent should be localised.

Moreover, although the statigraphic succession of the Faete edifice is exposed for several dozens of metres inside the craters of the Albano and Nemi Maars—both carved within the southern slope of the former stratovolcano—none of the four hydromagmatic units is detectable among the Faete suite, indeed represented only by lava flows and strombolian scoria-fall layers.

From the above considerations and in the light of the data presented in this paper, we conclude that the hypothesis of an origin of the DUs in the Campi di Annibale area should be ruled out.

4.2. A reappraisal of the energetic parameters and eruptive and post-eruptive scenarios

The identification and characterisation of the mid-distal Albano Maar deposits over a distance exceeding 100 km from the vent, indeed provide evidence of notably higher explosivity for the related volcanic eruptions than any previous evaluation. The present study also provides new relevant field data for a preliminary qualitative and semi-quantitative reassessment of the Albano eruptive scenarios, which, in our opinion, until now have been strongly conditioned by the poor knowledge on the mid-distal products (e.g. Giordano et al., 2002a; Porreca et al., 2003 on the Peperino Albano eruption).

A first important qualitative indication concerns the hierarchy of the Albano Maar eruptions, in terms of intensity and possibly magnitude of the seven explosive events. Indeed, our data point out that only the first, third, fifth and seventh eruptions produced high eruptive columns and/or pyroclastic currents sufficiently energetic to transport and deposit thick fall/surge deposits at several kilometres from the vent.

Significantly, these four, most intense eruptions are those that at near-vent sections comprise one or more fall layers in their internal stratigraphy. By comparison, the deposits of the three units which did not reach long distance, are systematically dominated by pyroclastic surge lithofacies. A further difference between the two cluster of eruptions is the degree of fragmentation of the juvenile clasts, which is appreciably higher in the deposits of the three, less disperded units. Both these features suggest a different extent of the magma–water interaction and hence distinct eruptive mechanisms. Apparently, the four larger explosive events had a more magmatic vs. hydromagmatic style, although this aspect needs more detailed investigation. In this regard, particularly significant are the compositional and textural features of the basal fallout layer of the last eruption of the Albano Maar (DU4 or ***f***), which is made up exclusively by idiosyncratic pumice and scoria likely resulting from dominantly magmatic fragmentation, as well as the abundance of vesicular juvenile clasts in the other DUs, showing similar magmatic characters. It must also be noted that, compared to purely magmatic explosions, in hydromagmatic ones a larger fraction of the thermal energy of the magma is converted in mechanical work (fragmentation), thus leaving less heat available for the development of a convective plume.

On the basis of the present available field data, a preliminary, quantitative evaluation of the eruptive parameters may be proposed only for the last, and possibly most powerful, eruption of the widespread DU4 or ***f***. Within its internal sequence, the fallout deposits of subunit DU4c show the widest areal dispersion and possibly represent the most energetic sustained eruption column event in the Albano eruptive history. Therefore, thickness and maximum lithic clast size measurements for this marker horizon, yielding isopach and isopleth maps (Fig. 9), provide a quantitative estimate of the eruptive parameters for the climactic, and possibly the most recent, eruptive episode of the Albano Maar. Following the method of Carey and Sparks (1986), the maximum column height is estimated at 18–21 km, the wind velocity at 20–25 m/s, and the corresponding peak magma discharge rate at c. $1.0 \times 10^4\,m^3/s$ (c. $2.6 \times 10^7\,kg/s$). On these grounds, a V.E.I. = 4 (Volcanic Explosivity Index; Newhall and Self, 1982) and a subplinian character can be attributed to this late eruptive phase (Fig. 10).

Although being not really well constrained, isopachs and lithic isopleths are broadly consistent with a vent area located in the south-eastern part of the present Albano Lake, and indicate an ENE-trending dispersal axis. Actually, the vent location may be better constrained by considering the whole litostratigraphic characters of the proximal equivalent unit ***f***, which indeed shows its maximum dispersion, thickness and clast size along the northern rim of the south-eastern sector of the Albano Maar, consistent with isopach and isopleth maps (Fig. 9) and previous inferences on the source area of unit ***f*** (Freda et al., 2006a).

By considering the maximum juvenile clast size of the coeruptive basal fallout deposits (subunit DU4a and its proximal equivalent level ***f*–1**) and their sharp thickness decay, a strombolian-like fountaining style may be

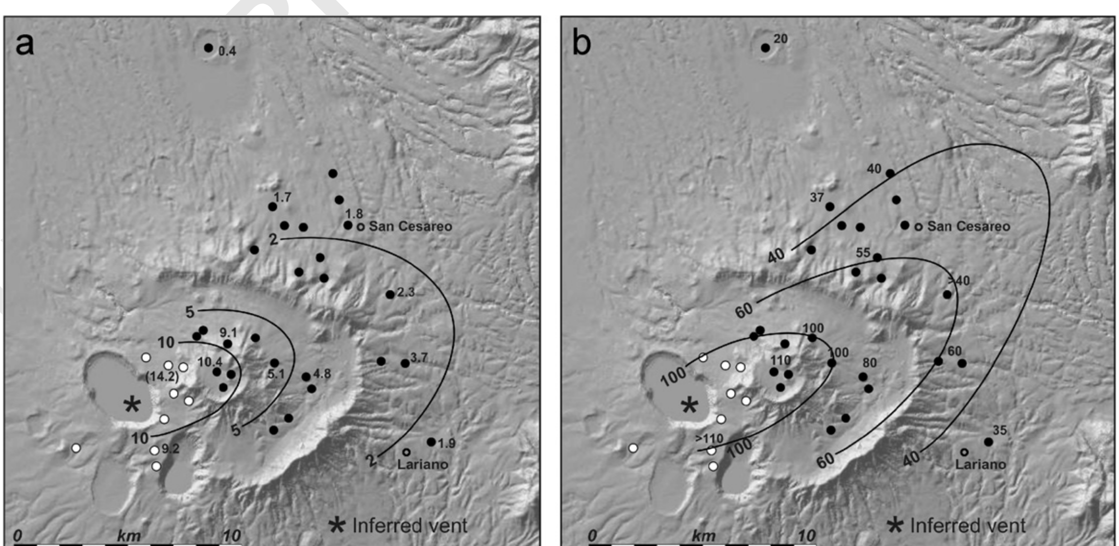

Fig. 9. Lithic isopleth (a) and isopach (b) maps (in cm) of the Albano distal subunit 4c (DU4c) corresponding to the proximal subunit ***f*–2**.

Please cite this article as: Giaccio, B., et al., Mid-distal occurrences of the Albano Maar pyroclastic deposits and their relevance for reassessing the eruptive scenarios of the most recent activity at the.... Quaternary International (2006), doi:10.1016/j.quaint.2006.10.013

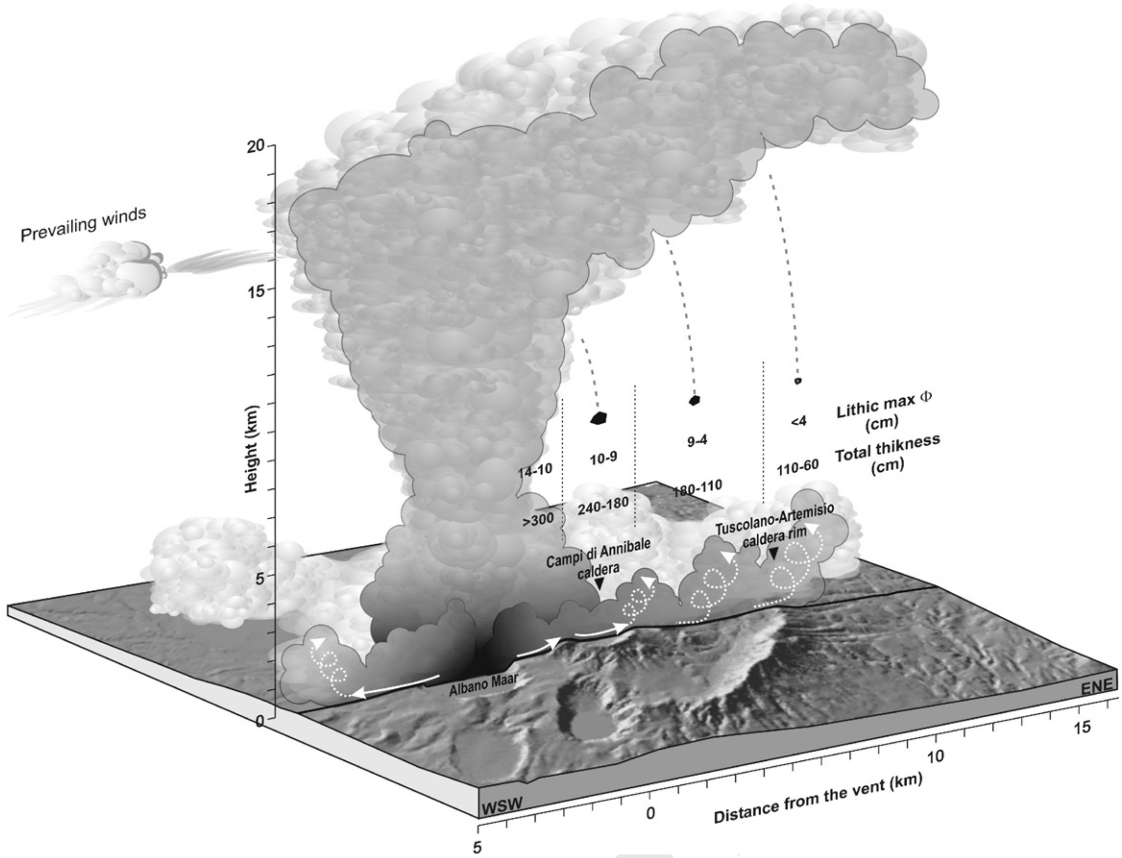

Fig. 10. Schematic reconstruction of the climactic stage of the Albano Maar eruption related to the distal unit 4 (DU4) equivalent to the proximal unit *f*.

attributed to the earliest, almost purely magmatic stage of this eruption.

Different from the early and late eruptive phases, the overall characters of subunit DU4b, e.g. its low-angle to plane-parallel stratification (Fig. 5), indeed indicate that the intermediate stage of the eruption was dominated by the formation of pyroclastic currents. Although the quantitative modelling of this stage is beyond the purpose of the present work, field evidence suggests that highly mobile, dilute, turbulent pyroclastic currents were able to surmount high topographic obstacles, such as Mt. Faete, as well as the inner Tuscolano-Artemisio caldera wall further downcurrent. Deposition occurred via traction and/or suspension sedimentation from the main current bodies and/or from associated lofting ash clouds up to notable distance from the vent, possibly exceeding 15 km.

The final stage of the eruption is represented only in the proximal area by the uppermost massive, matrix-supported deposits of unit ***f*** (layer ***f*–3**; Fig. 2), laid down by concentrated pyroclastic currents with shorter runout. Summarising, this eruption may be schematically described by four main stages, as follows: (1) strombolian-like fountaining phase (DU4a); (2) base surge phase (DU4b); (3) subplinian, sustained column phase (Du4c); (4) proximal deposition of either primary or secondary mass flows (***f*–3**).

From isopach map, following Fierstein and Nathenson (1992) and taking into account the Central Apennine occurrence as well, the deposit volume of subunit DU4c can be conservatively estimated at 0.25 km^3 (loose material). Also by including DU4a and DU4b, as well as near-vent deposits (unit ***f***), the value of c. 0.4 km^3 may be regarded as a plausible, minimum estimate of the total deposit volume.

With respect to the preceding Albano eruptions, the relatively sparse occurrence of the pertinent distal deposits (i.e., DU1, DU2 and DU3) does not allow at present time to quantify the related energetic eruptive parameters. However, some preliminary, qualitative evaluations may be drawn. All these units show textural features indicating a fallout origin. Locally, DU2 may show some characteristics of pyroclastic surge deposits, but these occur only at sections located at few kilometres from the crater rim (e.g. site n. 3 in Fig. 1). Thickness and maximum clast size data for the three units are broadly comparable to those for the fallout layer DU4c (cf. DU3 and DU1; Fig. 4), suggesting similar eruption intensities and magnitudes. Therefore, the eruptive parameters determined for the subunit DU4c may be regarded as a valid surrogate of the preceding three events.

Besides its direct implications on the definition of the eruptive scenarios, our reappraisal of the intensity and magnitude of the last Albano eruption and, possibly, of the

Please cite this article as: Giaccio, B., et al., Mid-distal occurrences of the Albano Maar pyroclastic deposits and their relevance for reassessing the eruptive scenarios of the most recent activity at the.... Quaternary International (2006), doi:10.1016/j.quaint.2006.10.013

other three major explosive events, provides new insights on the post-eruptive scenario. All distal units include abundant secondary volcaniclastic deposits, most channelled in paleo-depressions. Morphostratigraphic evidence suggests that the accumulation of voluminous reworked products may have strongly interfered with the local hydrological network, by filling depressions and triggering a rapid rising of the level of pre-existing lakes (e.g., Tuscolano-Artemisio caldera depression) and/or marked adjustment of the watercourses. Previous recognitions of similar channelled deposits in the north- and south-west area of the Colli Albani (Giordano et al., 2002b; Funiciello et al., 2003) indeed extend the zone of their potential impact, including the suburbs of Rome. Moreover, even if the distal units may simply hide Mousterian sites, we cannot exclude that the paucity of these sites in the dispersal area of the Albano units may reflect a deliberate response of local populations to the primary and secondary effects of volcanic activity. All the above observations suggest that, in analogy with what widely reported in the literature about very recent eruptions, the reworking of loose ash after the Albano Maar eruptions caused significant changes in the hydrological setting all over their depositional area, with possible, short term, major alterations of the local ecosystem with potential impact on the Palaeolithic groups.

5. Conclusion

The data set reported in this paper extends significantly the previously supposed area affected by an appreciable thickness of the pyroclastic deposits related to the most recent volcanic activity at the Colli Albani Volcanic District, dated between 70 and 36 ka B.P. According to this study, the north-eastern dispersion limits of the first, third, fifth and seventh eruptive units of the seven explosive events from the Albano multiple Maar should be shifted to at least 12 km more distally than thought until recently. The identification of these previously unrecognised Albano distal units, which was principally achieved by self-consistent, compelling tephrostratigraphic evidence, was strongly supported by petrological and geochemical isotope analyses, as well as by indirect chronological clues.

Contrary to any previous assessment, it is now evident that the Albano Maar activity was not limited to short-reaching hydromagmatic explosions, but also included far-reaching surge clouds and high, sustained column phases, subplinian in intensity. The last eruption, dated at c. 36 ka according to the available $^{40}Ar/^{39}Ar$ determinations, was possibly the most powerful one. At its climax the eruption column rose at a height of about 18–21 km and distributed pyroclastic material as far as the inner Apennine chain. Moreover, it was, unique among the recognised events, associated to the generation of highly mobile pyroclastic currents able to surmount high relief and leave deposits at distance exceeding 15 km from the vent. In a prospective of hazard evaluation, in addition to the potential direct eruptive impact, several lines of evidence presented in this paper suggest the occurrence of non negligible, or even severer, secondary effects on the hydrographic network related to the remobilization of the voluminous, loose volcanic products and their accumulation in valleys.

In the light of the recent redefinition of the state of activity of the Colli Albani Volcanic District from extinct to quiescent, our new findings may be crucial for the definition of future, expected eruptive scenarios. A management and mitigation plan of the volcanic hazard for the densely urbanized area of the Colli Albani and neighbouring Rome metropolitan area, should be drawn accordingly.

Finally, on a broader methodological plane, our results indeed show how a multidisciplinary and multi-scale, from local to regional, approach may be crucial not only when dealing with very large eruptions, but also to better understand the dynamics of minor, yet highly explosive, activities of multiple-maar volcanoes.

Acknowledgements

This article is a contribution of project "V3_1_13—Colli Albani", supported by "Istituto Nazionale di Geofisica e Vulcanologia" and by "Dipartimento per la Protezione Civile". We thank Guido Giordano and Roberto Isaia for useful discussions and sharing observations and opinions in the field. Many thanks to Donatella de Rita for her thoughtful revision and suggestions which substantially improved an early version of the manuscript.

We are grateful to Donatella Magri for giving us the opportunity to sample the tephra layer from the Castiglione lacustrine core, Pamela Cerino and Giuseppe Pulitani for their support on field and Marcello Serracino for his professional and kind assistance in performing the microprobe analyses at the Istituto di Geologia Ambientale e Geoingegneria laboratory, Rome.

Appendix A. Analytical methods

Major elements analyses—Major elements analyses of the glasses and clinopyroxene crystals were performed at the CNR-Istituto di Geologia Ambientale e Geoingegneria (Rome, Italy) with a Cameca SX50 electron microprobe equipped with five wavelength-dispersive spectrometers, using 15 kV accelerating voltage, 15 nA beam current, 10 μm beam diameter, and 20 s counting time. The following standards were used: wollastonite (Si and Ca), corundum (Al), diopside (Mg), andradite (Fe), rutile (Ti), orthoclase (K), jadeite (Na), barite (Ba), celestine (Sr), F-phlogopite (F), baritina (S), and metals (Cr and Mn). Ti and Ba contents were corrected for the overlap of the Ti K_α and BaK_α peaks.

$^{87}Sr/^{86}Sr$ *ratio*—Clinopyroxene crystals for Sr isotopic analysis were hand picked and, before dissolution, the samples were cleaned in dilute HF and HCl (approximately 5% each) for 10 min by an ultrasonic bath. The acid

Please cite this article as: Giaccio, B., et al., Mid-distal occurrences of the Albano Maar pyroclastic deposits and their relevance for reassessing the eruptive scenarios of the most recent activity at the.... Quaternary International (2006), doi:10.1016/j.quaint.2006.10.013

solution was then decanted by a pipette, and the separate repeatedly rinsed with de-ionised water. The separates were then dried, and dissolved in closed Savilex Teflon vials with a mixture of concentrated HNO_3 and HF on a hotplate. The samples were then dried down and taken up in concentrated HNO_3 and several drops of $HClO_4$ and dried down once again. The Sr has been separated on small columns of Sr specific resin (dowex 50 ×, 200–400 meshes) and loaded. The sample Sr was diluted with bidistilled water, dried down with a drop of $HClO_4$ in preparation for loading with tantalum chloride solution on an outgassed W filament for thermal ionisation mass spectrometric analysis. Samples were analysed for Sr isotopic composition on a VG 54 E (at CNR Istituto di Geologia Ambientale e Geoingegneria) single collector mass spectrometer using a multidynamic analysis routine, with normalization to 86Sr/88Sr = 0.1194. The average $^{87}Sr/^{86}Sr$ measured for NBS 987 over the period of analysis was 0.710241 ± 0.000020 2σ ($n = 15$).

References

Ayuso, R.A., De Vivo, B., Rolandi, G., Seal II, R.R., Paone, A., 1998. Geochemical and isotopic (Nd–Pb–Sr–O) variations bearing on the genesis of volcanic rocks from Vesuvius, Italy. Journal of Volcanology and Geothermal Research 82, 53–78.

Barbieri, M., Cavarretta, G., Romoli, L., Voltaggio, M., 1998. Tephra layers in Piana del Fucino (Central Italy) sediments: a provenance and U-Th chronology study. Tephrochronology and coesistence humans-volcanoes, Brives Charensac, Haute-Loire, August 24–29. Extended abstract.

Carey, S., Sparks, R.S.J., 1986. Quantitative models of the fallout and dispersal of tephra from volcanic eruption columns. Bullettin of Volcanology 48, 109–125.

De Rita, D., Funiciello, R., Parotto, M., 1988. Carta geologica del Complesso vulcanico dei Colli Albani. Progetto Finalizzato 'Geodinamica', C.N.R., Rome, Italy.

De Rita, D., Faccenna, C., Funiciello, R., Rosa, C., 1995a. Stratigraphy and volcano-tectonics. In: Trigila, R. (Ed.), The Volcano of the Alban Hills. Università degli Studi di Roma "La Sapienza", Rome, Italy, pp. 33–71.

De Rita, D., Giordano, G., Rosa, C., Sheridan, M.F., 1995b. Volcanic hazard at the Alban hills and computer simulations. In: Trigila, R. (Ed.), The Volcano of the Alban Hills. Università degli Studi di Roma "La Sapienza", Rome, Italy, pp. 267–283.

Demangeot, J., 1965. Geomorphologie des Abruzzes adriatiques in Memorie set Documents. Editions du Centre National de la Recherche Scientifique, Paris, p. 388.

Fairbanks, R.G., Mortlock, R.A., Chiu, T.-C., Cao, L., Kaplan, A., Guilderson, T.P., Fairbanks, T.W., Bloom, A.L., Grootes, P.M., Nadeau, M.-J., 2005. Radiocarbon calibration curve spanning 0–50,000 years BP based on paired $^{230}Th/^{234}U/^{238}U$ and ^{14}C dates on pristine corals. Quaternary Science Reviews 24, 1781–1796.

Fierstein, J., Nathenson, M., 1992. Another look at the calculation of fallout tephra volumes. Bullettin of Volcanology 54, 156–167.

Follieri, M., Magri, D., Sadori, L., 1988. 250,000 year pollen record from Valle di Castiglione (Roma). Pollen et Spores 30, 329–356.

Fornaseri, M., Cortesi, C., 1989. Recenti acquisizioni sull'età del Peperino di Albano. Documenta Albana, II Series 11, 7–10.

Freda, C., Gaeta, M., Karner, D.B., Marra, F., Renne, P.R., Taddeucci, J., Scarlato, P., Christensen, J., Dallai, L., 2006a. Eruptive history and petrologic evolution of the Albano multiple maar (Alban Hills, Central Italy). Bulletin of Volcanology 68, 567–591.

Freda, C., Gaeta, M., Karner, D.B., Marra, F., Renne, P.R., Taddeucci, J., Scarlato, P., Christensen, J., Dallai, L., 2006b. Erratum "Eruptive history and petrologic evolution of the Albano multiple maar (Alban Hills, Central Italy)". Bulletin of Volcanology 69, 115.

Funiciello, R., Giordano, G., De Rita, D., Carapezza, M.L., Barberi, F., 2002. L'attività recente del cratere del Lago di Albano di Castelgandolfo. Rendiconti dell'Accademia dei Lincei, Scienze Fisiche e Naturali 13 (9), 113–143.

Funiciello, R., Giordano, G., De Rita, D., 2003. The Albano maar lake (Colli Albani Volcano, Italy): recent volcanic activity and evidence of pre-Roman Age catastrophic lahar events. Journal of Volcanology and Geothermal Research 123, 43–61.

Gaeta, M., Freda, C., Christensen, J.N., Dallai, L., Marra, F., Karner, D.B., Scarlato, P., 2006. Evolution of the mantle source for ultrapotassic magmas of the Alban hills volcanic district (Central Italy). Lithos 86, 330–346.

Giordano, G., De Rita, D., Cas, R., Rodani, S., 2002a. Valley pond and ignimbrite veneer deposits in the small-volume phreatomagmatic 'Peperino Albano' basic ignimbrite, Lago Albano maar, Colli Albani volcano, Italy: influence of topography. Journal of Volcanology and Geothermal Research 118, 131–144.

Giordano, G., De Rita, D., Fabbri, M., Rodani, S., 2002b. Facies associations of rain-generated versus crater lake-withdrawal lahar deposits from Quaternary volcanoes, central Italy. Journal of Volcanology and Geothermal Research 118, 145–159.

Giordano, G., De Benedetti, A.A., Diana, A., Diano, G., Gaudioso, F., Marasco, F., Miceli, M., Mollo, S., Cas, R.A.F., Funiciello, R., 2006. The Colli Albani mafic caldera (Roma, Italy): stratigraphy, structure and petrology. Journal of Volcanology and Geothermal Research 155, 49–80.

Giraudi, C., 1998. Late Pleistocene and Holocene lake-level variations in Fucino Lake (Abruzzo, Central Italy) inferred from geological, archaeological and historical data. In: Harrison, S.P., Frezel, B., Huckriede, U., Weiβ, M.M. (Eds.), Paleaeohydrology as Reflected in Lake-level Changes as Climatic Evidence for Holocene Times. Gustav Fischer Verlag, Stuttgart, pp. 1–17.

Giraudi, C., Frezzotti, M., 1997. Late Pleistocene glacial events in the central Apennines, Italy. Quaternary Research 48, 280–290.

Karner, D.B., Marra, F., Renne, P., 2001. The history of the Monti Sabatini and Alban hills volcanoes: groundwork for assessing volcanic-tectonic hazards for Rome. Journal of Volcanology and Geothermal Research 107, 185–219.

Khun, S.L., 1995. Mousterian Lithic Technology, An Ecological Perspective. Princeton University Press, Princeton, NJ, 203pp.

Marra, F., Karner, D.B., 2005. The Albano Maar (Alban hills volcanic district, Italy): active or dormant volcano? Il Quaternario 18 (2), 173–185.

Marra, F., Freda, C., Scarlato, P., Taddeucci, J., Karner, D.B., Renne, P.R., Gaeta, M., Palladino, D.M., Trigila, R., Cavarretta, G., 2003. Post-caldera activity in the Alban hills volcanic district (Italy): $^{40}Ar/^{39}Ar$ geochronology and insights into magma evolution. Bulletin of Volcanology 65, 227–247.

Marra, F., Taddeucci, J., Freda, C., Marzocchi, W., Scarlato, P., 2004. The recurrence of volcanic activity along the Roman Comagmatic Province (Tyrrhenian margin of Italy) and its tectonic significance. Tectonics 23, TC4013.

Miccadei, E., Barberi, R., Cavinato, G.P., 1999. La geologia quaternaria della Conca di Sulmona (Abruzzo, Italia centrale). Geologica Romana 34, 31–50.

Narcisi, B., 1994. Caratteristiche e possibile provenienza di due livelli piroclastici nei depositi del Pleistocene superiore della Piana del Fucino (Italia centrale). Rendiconti dell'Accademia dei Lincei, Scienze Fisiche e Naturali 5 (9), 115–123.

Narcisi, B., Vezzoli, L., 1999. Quaternary stratigraphy of distal tephra layers in the Mediterranean—an overview. Global and Planetary Change 21, 31–50.

Please cite this article as: Giaccio, B., et al., Mid-distal occurrences of the Albano Maar pyroclastic deposits and their relevance for reassessing the eruptive scenarios of the most recent activity at the.... Quaternary International (2006), doi:10.1016/j.quaint.2006.10.013

Newhall, C.G., Self, S., 1982. The volcanic explosive index (VEI): an estimate of explosive magnitude for historical volcanism. Journal of Volcanology and Geothermal Research 87, 1231–1238.

Pappalardo, L., Civetta, L., D'Antonio, M., Deino, A., Di Vito, M., Orsi, G., Carandente, A., de Vita, S., Isaia, R., Piochi, M., 1999. Chemical and Sr-isotopical evolution of the Phlegraean magmatic system before the Campanian Ignimbrite and the Neapolitan Yellow Tuff eruptions. Journal of Volcanology and Geothermal Research 91, 141–166.

Paterne, M., Guichard, F., Labeyrie, J., 1988. Explosive activity of the south Italian volcanoes during the past 80,000 years as determined by marine tephrochronology. Journal of Volcanology and Geothermal Research 34, 153–172.

Peccerillo, A., 2001. Geochemistry and petrogenesis of quaternary magmatism in central-southern Italy. Geochemistry International 6, 579–592.

Rolfo, M.F., Giaccio, B., Sposato, A., in press. Siti del Paleolitico medio nell'area dei Colli Albani e loro contesto morfologico e pedotefrostratigrafico. Atti dalla XL Riunione Scientifica dell'Istituto Italiano di Preistoria e Protostoria: Strategie di Insediamento fra Lazio e Campania in età Preistorica e Protostorica, Roma, Napoli, Pompei 30 novembre—3 dicembre 2005.

Soligo, M., Tuccimei, P., Giordano, G., Funiciello, R., De Rita, D., 2003. New U-series dating of a carbonate level underlying the Peperino Albano phreatomagmatic ignimbrite (Colli Albani, Italy). Il Quaternario 16, 115–120.

Trigila, R., Agosta, E., Currado, C., De Benedetti, A.A., Freda, C., Gaeta, M., Palladino, D.M., Rosa, C., 1995. Petrology. In: Trigila, R. (Ed.), The volcano of the Alban Hills. Università degli Studi di Roma "La Sapienza", Rome, pp. 95–165.

Villa, I.M., Calanchi, N., Dinelli, E., Lucchini, F., 1999. Age and evolution of the Albano crater lake (Roman Volcanic Province). Acta Vulcanologica 11 (2), 305–310.

Wulf, S., Kraml, M., Brauer, A., Keller, J., Negendank, J.F.W., 2004. Tephrochronology of the 100 ka lacustrine sediment record of Lago Grande di Monticchio (southern Italy). Quaternary International 122, 7–30.

Table 1

Schematic stratigraphic succession and age of the proximal pyroclastic products of the Albano Maar correlated with their distal equivalent units (DUs). A comparison with previous stratigraphic subdivision of De Rita et al. (1995a) is also shown.

PROXIMAL AREA				**DISTAL AREA (NE)**
De Rita et al., 1995a	**Freda et al., 2006a-b (with updating)**			**This study**
Stratigraphy	**$^{40}Ar/^{39}Ar$ age (ka B.P.)**	**Eruptive cycles**	**Stratigraphy**	**Stratigraphy**
			Present, deep soil	Present, deep soil
	35.9±0.6		Unit ***f***	Albano DU4
			Incipient paleosol	
V Unit *Peperino Albano*	36.1±0.3 40.9±0.8		Unit ***e*** *Lapis Albanus*	Shallow paleosol
		Late	Incipient paleosol	
			Unit ***d***	Albano DU3
paleosol			Moderately deep paleosol	
IV Unit	41.2±1.1		Unit ***c***	Deep paleosol
paleosol			Deep paleosol	
III Unit	68.6±1.1		Unit ***b***	Albano DU2
paleosol			Shallow paleosol	
II Unit		Early	Unit $\boldsymbol{b}_{\alpha}$	Shallow paleosol
paleosol			Shallow paleosol	
I Unit	69.4±0.6		Unit ***a***	Albano DU1
			Very deep paleosol on Faete Phase or Ariccia Maar products	Very deep paleosol on Faete Phase products

Table 4

$^{87}Sr/^{86}S$ analyses of clinopyroxene crystals of the investigated distal units (DUs) compared with similar known values for the Albano Maar proximal units and some eruptive units representative of the three main phases of the Colli Albani Volcanic District. A significant consistence between the values of the DUs and the Albano Maar deposits can be noted.

Site	Sample	Phase	Unit	Age (ka)	87Sr/86Sr	±2σ
A3	CES-2		Distal tephra	45-30	0,70969	2×10^{-5}
2	CA-A4c	(**LH**)[a]	DU4c	***LG***[b]	0.70958	2×10^{-5}
	CA-A4a		DU4a		0.70957	2×10^{-5}
1	S-A4c		DU4c		0.70953	2×10^{-5}
	S-A4a		DU4a		0.70953	2×10^{-5}
	S-A3d		DU3d		0.70959	2×10^{-5}
	S-A3c		DU3c		0.70963	2×10^{-5}
	S-A2b		DU2b		0.70963	2×10^{-5}
3	B-A3d		DU3d		0.70955	2×10^{-5}
5	L-A1		DU1		0.70950	2×10^{-5}
8	CAS		DU4c	36-35[c]	0.70945	2×10^{-5}
9	SCI-f	**LH**	AL(***f-1/2***)	36	0.70953	2×10^{-5}
10	PC-d2		AL(***d-2***)	41-36	0.70967	2×10^{-5}
14	AH-17, 1*		AL(***f-1/2***)	36	0.709544	1×10^{-5}
	AH-3C16/4Fb*		AL(***f-1/2***)	36	0.709579	1×10^{-5}
Albano Lake (12)	AH-3A, 5*		AL(***a-1***)	69	0.708508	1×10^{-5}
	AH-3A, 4*		AL(***a-1***)	69	0.709416	0.9×10^{-5}
15	AH-9, 5*		AL	41	0.709621	0.9×10^{-5}
	AH-9, 4*		AL	41	0.709675	0.9×10^{-5}
	AH-1D*		AR	204	0.710109	1.3×10^{-5}
4	CAR-F	**F**	PSC	-	0,71031	2×10^{-5}
13	AH-7A*		MM	308	0.710304	0.9×10^{-5}
	AH-7*		MM	308	0.710382	0.9×10^{-5}
	UFU*	**T-A**	VS	366	0.710506	1×10^{-5}
	PN*		PN	407	0.710543	0.9×10^{-5}
	PR*		PR	457	0.710654	0.9×10^{-5}
	T*		LV	460	0.710643	1.4×10^{-5}
	TP*		TP	528	0.710893	0.9×10^{-5}
	P*		TTC	561	0.711069	1×10^{-5}
	C4*		CA	608	0.711200	0.9×10^{-5}

[a] According to the tephrostratigraphic correlation (see section 3.1.2. for details).

[b] Inferred from morpho-pedostratigraphic and archaeological setting (see section 3.1.4. for details).

[c] According to the age model for the Castiglione lacustrine pollen record (Follieri et al., 1988).

* Data from Gaeta et al. (2006).

Abbreviations: ***LG***: Last Glacial period; **LH**: Late Hydromagmatic; **F**: Faete; **T-A**: Tuscolano-Artemisio; AL: Albano Maar (in brackets related units/subunits); AR: Ariccia Maar; PSC: Peri-caldera scoria cone; MM: Mt. Mellone lava flow; VS: Villa Senni Eruptive Unit; PN: ozzolane nere; PR: Pozzolane Rosse; LV: Vallerano lava flow; TP: Tufo del Palatino; TTC: Trigoria-Tor de' Cenci Tuff; CA: Cave fall layer.